Title: Long-lasting stem cell-like memory CD8+ T cells with a naïve-like profile upon yellow fever vaccination.

Authors: Fuertes Marraco SA, Soneson C, Cagnon L, Gannon PO, Allard M, Abed Maillard S, Montandon N, Rufer N, Waldvogel S, Delorenzi M, Speiser DE

Journal: Science translational medicine

Year: 2015 Apr 8

Issue: 7

Volume: 282

Pages: 282ra48

DOI: 10.1126/scitranslmed.aaa3700

Long-lasting stem cell-like memory CD8 T cells with high "Naïveness" upon Yellow Fever vaccination

One Sentence Summary:

The Yellow Fever vaccine induces a CD8 T stem cell-like memory subset that preserves a high degree of "Naïveness" and is stably maintained for over two decades in humans.

Authors:

Silvia A. Fuertes Marraco[1,2], Charlotte Soneson[3], Laurène Cagnon[2], Philippe O. Gannon[2], Mathilde Allard[2], Samia Abed Maillard[2], Nicole Montandon[2], Nathalie Rufer[2], Sophie Waldvogel[4], Mauro Delorenzi[1,2,3], Daniel E Speiser[1,2].

1. Ludwig Cancer Center, University of Lausanne, Switzerland
2. Department of Oncology, Lausanne University Hospital (CHUV), Switzerland
3. Bioinformatics Core Facility, SIB Swiss Institute of Bioinformatics, Lausanne, Switzerland
4. Service Vaudois de Transfusion Sanguine de la Croix Rouge, Lausanne, Switzerland.

Correspondence:

Dr. Daniel E. Speiser

Clinical Tumor Biology & Immunotherapy Group.
Ludwig Cancer Center, University of Lausanne
Hôpital Orthopédique HO-05/1553
Av. Pierre-Decker 4
CH-1011 Lausanne, Switzerland
doc@dspeiser.ch

Abstract:

Efficient and persisting immune memory is essential for long-term protection from infectious and malignant diseases. The Yellow Fever (YF) vaccine is a live-attenuated virus that mediates life-long protection, with recent studies showing that the CD8 T cell response is particularly robust. Yet limited data exists regarding the long-term CD8 T cell response, with no studies beyond five years post-vaccination.

Hereby, we investigated 41 vaccinees, spanning 0.27 to 35 years after vaccination. YF-specific CD8 T cells were readily detected in almost all donors (38/41), with frequencies decreasing with time. As previously described, effector cells dominated the response early after vaccination. We detected a population of Naïve-like YF-specific CD8 T cells that was stably maintained for over 25 years and was capable of self-renewal *ex vivo*. In-depth analyses of markers and genome-wide mRNA profiling showed that Naïve-like YF-specific CD8 T cells in vaccinees: i) were distinct from genuine Naïve cells in unvaccinated donors ii) resembled the recently described stem cell-like memory subset (Tscm), and iii) amongst all differentiated subsets, had profiles closest to the Naïve. Our findings reveal that CD8 Tscm are efficiently induced by a vaccine in humans, persist for decades and preserve a particularly high degree of "Naïveness". This supports YF vaccination as an optimal mechanistic model for the study of long-lasting memory CD8 T cells in humans.

Main Text:

Introduction

Cytotoxic CD8 T cells are key to the destruction and clearance of pathological cells that harbor intracellular infections or aberrant alterations such as tumors. Therefore, CD8 T cells are at the center stage in the design of immunotherapeutic strategies to fight cancer and chronic infectious diseases. Compared to established therapies (chemo- or radio-therapies), a major advantage of immunotherapy lies in the "memory" quality of adaptive immune responses, with potential for long-term and recall effects. Great efforts are ongoing to better understand the mechanisms underlying the development and long-term maintenance of memory for protection from disease *(1-5)*.

The study of human (CD8) T cell responses has largely relied on anti-viral responses to highly prevalent or medically relevant viruses. These conventional references include the lifelong persisting herpes viruses Cytomegalovirus (CMV) and Epstein-Barr Virus (EBV), the acute and seasonal Influenza (Flu) virus, and chronic viruses that cause severe pathology such as Hepatitis C Virus (HCV) and Human Immunodeficiency Virus (HIV) *(6)*. For instance, the "CEF" (CMV, EBV, Flu) peptide pool is amongst the most frequently used positive controls to monitor human CD8 T cells *(7)*. However, these viral specificities correspond to infections that are difficult to track in terms of the timing of the exposure to the pathogen, including recurrence in the case of chronic infections. Conversely, active

vaccination offers a scenario of synchronized and supervised induction of the immune response. As such, vaccines represent, in practice, the best available models for the controlled study of an immune response in humans *(8)*.

While prevention of infection *per se* is primarily guaranteed by the induction of neutralizing antibodies, the cytotoxic CD8 T cell responses are of particular importance in the clearance of pathogens *(9)*. Several vaccines, and in particular live attenuated formulae such as the Yellow Fever (YF) and Smallpox vaccines, induce robust T cell responses considered as major contributors to the protection conferred by vaccination *(8, 10)*. The live attenuated YF vaccine (YF-17D and YF-17DD strains) stands out as one of the most successful in terms of public health impact, as well as the robustness and quality of the immune response elicited *(8, 10, 11)*. In use since 1937, the vaccine is known to induce neutralizing antibodies that persist at least up to 38 years *(12)*. In recent years, the YF-17D vaccine has also attracted major research interest for its capacity to induce a particularly strong CD8 T cell response. This response features high magnitude, broad specificity with overlapping epitopes spanning multiple HLA class I and class II motifs (conferring prevalent and high immunogenicity in the human population), polyfunctionality, high proliferative potential and long-term persistence *(13-16)*. In addition, the particular innate response to the live attenuated virus may contribute to the success of the YF vaccine, featuring the activation of multiple dendritic cell subsets via several pattern recognition receptors to orchestrate such a competent adaptive immune response *(17-19)*.

Upon vaccination, there is a peak of viremia that resolves by day 15. The CD8 T cell response peaks between 14 and 30 days and can reach up to 10% of the circulating CD8 T cells even for a single specificity such as the NS4b$^{214\text{-}222}$ epitope *(13, 15, 16)*. In terms of the

differentiation phenotype, YF-specific CD8 T cells show an effector phenotype (CCR7- CD45RA-) very early in the response (day 14). However, CD45RA is re-expressed from day 30 onwards *(13, 16, 20)*. This EMRA population shows properties of polyfunctional memory cells (CD28+/-, CD27+, proliferation), which defies the conventional classification of EMRA (CCR7- CD45RA+) as terminally differentiated effector CD8 T cells *(10, 13, 16)*.

In the light of these recent reports, it has become apparent that YF vaccination induces a distinct activation and memory differentiation of human CD8 T cells that may explain its particular efficacy. However, reports so far have addressed the phenotype of YF-specific CD8 T cells with particular emphasis in the first 90 days after vaccine administration, and very limited data exists at later time-points. The EMRA phenotype for instance has been observed in limited numbers of donors and only up until 46 months after vaccination (13, 16, 20). In this study, we aimed to thoroughly characterize the memory CD8 T cells that persist in the long-term, in the range of decades following YF vaccination.

Results

The Yellow Fever vaccine 17D induces a Naïve-like population of antigen-experienced CD8 T cells that is stably maintained over 25 years

We studied a cohort of 41 healthy volunteers vaccinated with YF-17D, between 3 months and 35 years ago, including four individuals having received multiple vaccines (table S1). In order to detect YF-specific CD8 T cells, we used HLA-A*02 tetramers to stain cells bearing a TCR specific for the highly prevalent NS4b$^{214-222}$ epitope, hereafter referred as A2/NS4b (fig. 1 A) (13, 14, 16). A2/NS4b+ CD8 T cells were detected in the large majority of vaccinees, with only 3 / 41 donors having frequencies below 0.01% and considered negative (fig. 1 B). Remarkably, A2/NS4b+ CD8 T cells were detected over at least 25 years after vaccination, albeit at decreasing frequencies with time (fig. 1 B).

In order to study the differentiation status of YF-specific CD8 T cells, subsets were defined on the basis of the expression of conventional markers CCR7 and CD45RA, namely: Naïve (CCR7+ CD45RA+), CM (CCR7+ CD45RA-), EM (CCR7- CD45RA-) and EMRA (CCR7- CD45RA+) subsets (6), as indicated in fig. 1C. A2/NS4b+ CD8 T cells showed considerable heterogeneity in subset distribution amongst donors. Overall, only a few donors showed substantial CM populations, and the largest proportion of cells were found either in the EMRA subset or, surprisingly, falling within the conventional Naïve gate (fig. 1D and E). We hereafter termed these CCR7+ CD45RA+ A2/NS4b+ CD8 T cells “Naïve-like”, since they appeared in the conventional Naïve gate but their “genuine Naïve vs memory” nature was to be determined, as addressed throughout the experiments that follow. Moreover, we

observed that these A2/NS4b+ Naïve-like CD8 T cells displayed variable levels for CCR7 and CD45RA. There was either CCR7^{high} CD45RA^{high} expression (hereafter termed "Naïve^{high}"), or intermediate CCR7 and/or CD45RA expression (hereafter termed "Naïve^{int}"). The detailed gating is shown in fig. 1 C and D and quantified in fig. 1E.

Next, we addressed the relationship between the differentiation status of YF-specific CD8 T cells in relation to the years since vaccination. Of note, there was an inherent trend towards longer vaccine history corresponding to vaccinees of older age (fig. S1 A). Increasing age is known to correlate with fewer Naïve cells and slightly more differentiated cells (EM/EMRA) (fig. S1 B and C) (21, 22). In order to normalize inter-donor and age-related variations, we quantified the frequency of A2/NS4b+ CD8 T cells within each differentiation subset, rendering the data independent of the personal composition of subsets in Total CD8 T cells as well as independent of the age of donors (fig. S1 D).

YF vaccination induced a large population of differentiated CD8 T cells, comprising up to 6.45% of EMRA early after vaccination, that steadily decreased with time (fig. 2 A, panel "EMRA"; fig. 2 C, slope = -0.093). Although generally less frequent, the CM and EM populations detected also decreased with time (fig. 2 A, "EM" and "CM" panels), but less steeply (fig. 2 C). Interestingly, the population of Naïve-like A2/NS4b+ CD8 T cells was also clearly increased in vaccinees compared to unvaccinated individuals, hinting that this Naïve-like population is mobilized by the vaccine (fig. 2 A, "Naïve" panel). Yet most strikingly, the frequency of Naïve-like A2/NS4b+ CD8 T cells was stably maintained over the years after vaccination, even after 25 years (fig. 2 C, slope = -0.014).

Further analysis of the A2/NS4b+ CD8 T cells within the conventional Naïve gate showed different behaviors for the Naïve^{high} *versus* the Naïve^{int} cells. The latter were sharply

induced by the vaccine, reaching frequencies up to 2.46%, with a slow but significant decrease with time (fig. 2 B, "Naïve^{int}" panel; fig. 2 C: slope -0.034). In contrast, the Naïve^{high} A2/NS4b+ CD8 T cells barely increased, only by an average 1.5-fold in vaccinated *versus* detectable unvaccinated donors (note also that most unvaccinated donors (7/10) had A2/NS4b+ frequencies below the detection limit of <0.01%). The Naïve^{high} A2/NS4b+ CD8 T cells also showed a strikingly flat time-course (fig. 2 B, "Naïve^{high}" panel, fig. 2 C: slope = -0.00009).

As an additional observation, the four vaccinees with a history of multiple vaccines (table S1) showed frequencies and phenotype of A2/NS4b+ CD8 T comparable to single-shot vaccinees (fig. 1 B and fig. 2).

Naïve-like YF-specific CD8 T cells induced by the YF-17D vaccine are distinct from genuine Naïve cells and resemble the stem cell-like memory subset

We next focused on the characterization of these newly identified Naïve-like CD8 T cells induced by vaccination with YF-17D. It was critical to evaluate the "memory" nature of such cells that fall in the conventional Naïve gate. Recently, a new memory subset that also co-expresses CCR7 and CD45RA has been reported and termed the stem cell-like memory (Tscm) subset *(23-25)*. Tscm have properties of differentiated cells yet retain high stemness and phenotypical proximity to Naïve cells – they were also originally described as "Naïve-like" before coining Tscm. We therefore performed a detailed characterization of YF-specific CD8 T cells with a two-fold focus: i) to address whether they are truly distinct from genuine Naïve cells and ii) to assess similarities to the recently reported Tscm subset.

We performed a thorough screen using a wide panel of markers to study YF-specific CD8 T cells amongst the characteristic profiles of the differentiation subsets. This panel included conventional and previously reported differentiation markers (CD27, CD28, CD45RO, IL-7Rα/CD127, CD62L, CCR5, Granzymes A and B, Perforin, BTLA, PD1, PDL1, KLRG1, 2B4 *(6, 26)*, markers that have been used to distinguish the stem cell-like memory subsets (CD58, CD95, CXCR3, IL-2Rβ/CD122, CD11a (alpha chain of LFA-1), CD161, IL-18Rα, ABC-B1 *(23, 25, 27, 28)*, markers that showed potential relevance in differentiation and migration (CCR4, CLA *(29)*, resident memory markers CD69 and CD103 *(30)*, activation markers HLA-DR, CD38 *(13, 16)*) and other related markers (IL-2Rα/CD25, IL-15Rα/CD215, ICOS). This wide marker screen was performed on a representative selection of 16 vaccinees, spanning up to 17 years after vaccination (fig. S2 A). As shown above, the majority of A2/NS4b+ cells were either EMRA or Naïve-like.

First, to assess whether the Naïve-like A2/NS4b+ CD8 T cells in vaccinees were truly distinct from genuine Naïve cells, A2/NS4b+ CD8 T cells in unvaccinated individuals were studied in more detail. This was technically challenging due to the low frequencies in unvaccinated individuals, which were generally close to the detection threshold of 0.01% of Total CD8 T cells (fig. 1 B). Analysis was nevertheless possible in five unvaccinated donors with sufficient A2/NS4b+ CD8 T cells (>35 cells detected) and showed that these fell in the Naïve gate (fig. 3 A and B). Pertinently, these also expressed CD28 and CD27 but did not express markers characteristic of the Tscm subset, notably CD58, CD95 and CXCR3 *(6, 23, 25, 27)* (fig. 3C and D). In contrast, Naïve-like A2/NS4b+ CD8 T cells from vaccinees did show positive expression for the Tscm markers CD58, CD95 and CXCR3 (fig. 3C and D). Therefore, the Naïve-like A2/NS4b+ CD8 T cells in vaccinees were truly distinct from genuinely Naïve A2/NS4b+ CD8 T cells found in unvaccinated individuals and rather

corresponded to the Tscm subset. In agreement, the Total Tscm subset was analyzed based on gating the minor population of cells expressing CD58 and CD95 within the Total Naïve population (fig. 3E). This showed a prominent population of A2/NS4b+ Tscm cells in vaccinees (average 0.98% A2/NS4b+ cells within Tscm) as opposed to unvaccinated individuals, where A2/NS4b+ cells were not detectable within Tscm (fig. 3F).

A wide variety of markers were further analyzed in vaccinees, comparing A2/NS4b+ CD8 T populations to the respective reference populations in Total CD8 T cells. In addition to CD58, CD95 and CXCR3 mentioned above, A2/NS4b+ Naïve-like CD8 T cells distinctly expressed IL-2Rβ, CD11a^{high}, KLRG1, Granzyme A, IL-18Rα and CD45RO, in clear contrast to the Total Naïve population (fig. 3 G and H). Interestingly, the profile of A2/NS4b+ EMRA cells was overall close to the Total EMRA population but displayed particularly elevated levels of CD28, CD27, IL-7Ra, CXCR3, CD62L, BTLA and IL-18Rα. The latter is in agreement with previous studies where YF vaccination was reported to raise a particular type of EMRA cells that defy the terminally differentiated phenotype generally attributed to the EMRA subset *(10, 13, 31, 32)*. While the majority of A2/NS4b+ CD8 T cells were Naïve-like or EMRA, there were sufficient events in EM and CM gates of A2/NS4b+ CD8 T cells in several donors for flow cytometry analyses; the complete data series, including the 31 markers and all detectable subsets are detailed in fig. S2 B. Considering the markers overall, it was only the A2/NS4b+ Naïve-like CD8 T cells that showed a significantly different profile as compared to the corresponding reference population (i.e. *versus* Total Naïve; Wilcoxon comparisons in fig. 3 H and fig. S2 B).

Additionally, in order to investigate changes over time since vaccination, we selected the eight markers that showed greatest differences between vaccine-induced A2/NS4b+ Naïve-

like CD8 T cells and the Total Naïve: CD58, CD95, CXCR3, KLRG1, CD11a^{high}, IL-18Ra, Granzyme A and IL-2Rb. The time-span of vaccination in the selection of 16 donors was ≈17.5 years. Considering the "years since vaccination" (fig. S2 C), the levels of all markers within Naïve-like A2/NS4b+ CD8 T cells had a slight tendency to decrease, statistically significant for IL-2Rb and CXCR3. The reference Total Naïve cells also displayed a tendency for lower CXCR3 and higher CD58 with time, pointing towards inter-donor variation for these two markers. Nevertheless, for the eight markers, the A2/NS4b+ Naïve-like cells expressed distinctly superior levels as compared to the Total Naïve population, even in the second decade after vaccination.

Naïve-like Tscm are also found in other viral antigen-specificities

T cells with various viral specificities and particular T cell differentiation stages have been thoroughly studied in humans and are frequently used as reference populations. These specificities pertain to relatively prevalent chronic or acute viral infections such as HCV, Flu, EBV, HIV and CMV, which, in this order, display increasing differentiation status*(6)*. In order to compare YF-specific CD8 T cells to other antigen specificities, we further analyzed the 16 donors for CD8 T cells specific for Flu, EBV and CMV (fig. 4). In addition, we studied Melan-A-specific CD8 T cells as a population of cells that displays a truly naïve quality in healthy donors not bearing melanoma nor diagnosed with vitiligo *(31, 32)*. All 16 vaccinees had detectable populations specific for Melan-A and Flu, 13 were positive for EBV, and 5 for CMV (fig. 4 B). As expected, Melan-A-specific CD8 T cells were predominantly Naïve, while Flu-, EBV- and CMV-specific CD8 T cells showed subset distributions with increasing differentiation (CM → EM → EMRA) (fig. 4 C). All specificities

showed cells falling in the conventional Naïve gate (fig. 4 A and C). Further analysis of CD58, CD95 and CXCR3 revealed that, within the Naïve gate, Melan-A-specific cells were mostly CD58- CD95- $CXCR3^{low}$, supporting the notion that these cells are genuinely Naïve. In contrast, all viral antigen-specific cells showed Naïve-like cells triple positive for CD58, CD95 and CXCR3, albeit at varying degrees. Flu-specific Naïve-like CD8 T cells were more variable depending on the donor, while EBV- and CMV-specific cells were particularly high in CD58 and CD95 expression. For CXCR3, YF- and CMV-specific CD8 T cells showed higher expression (fig. 4 D). Interestingly, Flu-specific Naïve-like CD8 T cells often showed a split population for CD58 and CD95. This may be due to the presence of both genuine Naïve and Naïve-like cells, presumably depending on the history of Flu vaccination and/or infection. The latter was however difficult to track in our donors, given the endemic nature of Flu worldwide.

Our data overall indicated that the Naïve-like subset was also detected in other viral specificities and generally differed from the reference Naïve population in total CD8 T cells and from self antigen-specific Naïve CD8 T cells.

In addition, we addressed whether Naïve-like CD8 T cells were also generated with specificities other than the HLA-A*02-restricted $NS4b^{214-222}$ (LLWNGPMAV). Previous studies using stimulation of YF vaccinee samples with peptide pools have shown that the CD8 T cell response can be diverse and highly variable across donors, yet HLA-A*02 positive donors consistently display responses to $NS4b^{214-222}$ *(13, 14, 16)*. In fact, only a limited number of epitopes other than A2/NS4b, or peptide pools activating vaccinee samples, have been described *(13, 14, 16, 20)*. Based on these studies and HLA-binding predictions (BIMAS and SYFPEITHI), we generated a selection of nonamer or decamer

epitopes alternative to the A2/NS4b that could potentially yield tetramer stainings in YF vaccinees. Following the HLA-typing information available in our cohort, we could test non-HLA-A*02 restricted epitopes: “B35/HPF” in three vaccinees, “B7/RPI” in four vaccinees and “A24/VYM” in one vaccinee; plus HLA-A*02 restricted epitopes in 25 vaccinees: “A2/AMD”, “A2/VML”, “A2/VCY” and “A2/GIL” (fig. S3). Of note, many vaccinees in our cohort did not have the appropriate HLA type to analyze the aforementioned selection of Yellow Fever epitopes. Out of 108 samples tested, this screen resulted in 4 positive samples (tetramer positive cells > 0.01% in total CD8 T cells), including two for “A2/VML” and two for “B7/RPI” (fig. S3 A). Analyses of these tetramer positive cells subsequently showed that B7/RPI+ CD8 T cells could also display a Naïve-like Tscm phenotype (falling in the conventional Naïve gate yet expressing CD58 and CD95) (fig. S3 B). Donor LAU 5005 had particularly high frequencies of Naïve-like B7/RPI+ CD8 T cells (90%) while the two A2/VML positive samples showed very few Naïve-like cells (0.5 – 2.8 %) (fig. S3 B). Nonetheless, the screen showed that Naïve-like Tscm subsets were also generated against epitopes other than A2/NS4b, in particular the B7/RPI. Together with the evidence on Naïve-like CD8 T cells found in other viral specificities (fig. 4), this shows that generation of Naïve-like Tscm is not exclusive to A2/NS4b+ CD8 T cells.

Naïve-like YF-specific CD8 T cells display mRNA profiles that are close to Tscm cells and with high preservation of “Naïveness”

In order to comprehend the global particularities of YF vaccine-induced Naïve-like CD8 T cells, we analyzed their genome-wide mRNA profile and compared it to the conventional subsets in total CD8 T cells. The latter included Naïve, CM and a pool of EM and EMRA

283 referred to as “Effectors”. We also analyzed the Tscm subset *(23, 25)*, gated as the minor
284 population expressing CD58 and CD95 within the Naïve gate of total CD8 T cells. These five
285 populations were isolated from each of eight selected vaccinees, spanning over 17 years of
286 vaccination history. The sorting strategy and the subset distribution of cells from vaccinees
287 are shown in fig. S4.
288
289 Most remarkably, principal component analysis clearly showed a gradient of differentiation
290 along the first principal component (PC1), from Naïve to a mixture of Tscm/CM to effectors.
291 Within this gradient, the A2/NS4b+ Naïve-like CD8 T cells clustered near the Tscm/CM
292 samples (fig. 5 A to C). Moreover, amongst all differentiated populations, A2/NS4b+ Naïve-
293 like CD8 T cells lied distinctly closest to the Naïve subset (fig. 5 A to C). These observations
294 were further confirmed quantitatively based on pairwise comparisons to calculate inter-
295 sample distances along PC1. The Naïve-like A2/NS4b+ CD8 T cells were most closely
296 related to the Tscm subset (fig. 5 D, left panel: “comparisons to A2/NS4b+ Naïve-like”). In
297 addition, the Naïve-like A2/NS4b+ CD8 T cells were closest in the comparison to the
298 reference Naïve subset (fig. 5 D, right panel: “comparisons to Total Naïve”). The Total Tscm
299 samples were generally found interspersed with the Total CM samples (fig. 5 B and C).
300 Pertinently, by considering the genesets that define “Differentiation” in CD8 T subsets as
301 well as the differences in “Tscm vs. Naïve” as described in the report of the Tscm subset
302 *(23)*, we could similarly observe that the A2/NS4b+ Naïve-like CD8 T cells were closely
303 clustered together and displayed a profile between the CM/Tscm and Naïve cells (fig. S4 E
304 and F).
305
306 Very few genes were significantly differentially expressed between the A2/NS4b+ Naïve-
307 like CD8 T cells and the Total Naïve, Total Tscm or Total CM, due to inter-sample variation

in the context of relatively small mRNA differences, and in contrast to the numerous significant genes in the comparison to the Total Effectors (table S3). The analysis of mRNA profiles altogether showed that contributions from large numbers of genes globally differentiated the various subsets. These global differences reflected a gradient of differentiation that suggests that the A2/NS4b+ Naïve-like CD8 T cells, amongst all differentiated subsets, have globally preserved most "Naïveness".

Long-term persisting YF-specific CD8 T cells respond to cognate peptide and show homeostatic proliferation with IL-15, with a proliferative advantage for the Naïve-like phenotype

As compared to Naïve cells that have never been primed, memory CD8 T cells readily respond to cognate antigen and are capable of homeostatic proliferation in presence of IL-15 *(23, 33)*. Therefore, we assessed the proliferation capacity of YF-specific CD8 T cells, and its link to the Naïve-like phenotype. Due to the limited bioavailability of samples (technical limitation detailed in discussion), we could not analyze individually isolated subsets of A2/NS4b+ CD8 T cells from large numbers of donors and stimulate with multiple conditions. We therefore first stimulated PBMC from vaccinees with the NS4b peptide in the presence of IL-2 or IL-15 or treated with either cytokine alone. PBMC from three unvaccinated individuals served as controls. Both in the presence of IL-2 or IL-15, A2/NS4b+ CD8 T cells from the large majority of vaccinees proliferated efficiently in response to cognate NS4b peptide (fig. 6A). Importantly, while IL-2 alone generally resulted in no expansion, IL-15 alone induced considerable expansion, demonstrating IL-

15-driven homeostatic proliferation characteristic of memory cells (fig. 6 A). Pertinently, the A2/NS4b+ CD8 T cells from the three unvaccinated individuals did not show proliferation, in agreement with their genuine Naïve status (fig. 6A).

In order to assess the link between the Naïve-like phenotype and proliferation capacity, the expansion was compared to the starting frequency of Naïve-like cells (fig. 6 B). In spite of the variability amongst samples, a higher starting frequency of Naïve-like cells significantly correlated with greater expansion in response to peptide and IL-15, and a tendency in this direction was seen with peptide and IL-2 ($p = 0.068$). Interestingly, a higher starting Naïve-like frequency was also significantly associated with greater homeostatic proliferation with IL-15 alone and with better survival with IL-2 alone (fig. 6 B). In addition, the capacity to respond to peptide was relatively stable long-term after vaccination, over 15 years after vaccination (fig. S5 A).

Naïve-like YF-specific CD8 T cells expanded *in vitro* generate effectors and show self-renewal

The defining property of stem cells is their capacity to self-renew *(34, 35)*. A fundamental question was therefore to assess the quality of the progeny of Naïve-like A2/NS4b+ CD8 T cells. To this end, Naïve-like A2/NS4b+ CD8 T cells were purified and expanded *in vitro*, in comparison to Non-Naïve counterparts. Since we started with very low numbers of cells, we stimulated with PHA, IL-2 and irradiated feeders, a protocol that is used for T cells cloning because it provides robust polyclonal stimulation. By day 14, sufficient cells were yielded to analyze the progeny generated from either Naïve-like (n=5) or Non-Naïve (n=4) A2/NS4b+ CD8 T cells. Both progenies displayed CCR7- effectors (fig. 6 C). The Non-Naïve

progeny showed a slightly increased population doubling and higher proportion of EM as opposed to EMRA in the progeny of Naïve-like (fig. S5 B to D). The effector progeny from Naïve-like showed loss of Naïve markers CD28, CD27 and IL-7Rα, demonstrating typical differentiation and not merely loss of CCR7 (fig. S5 B and E). Critically, the purified Naïve-like A2/NS4b+ CD8 T cells, and not the purified Non-Naïve, generated a small fraction of expanded cells that retained the Naïve-like phenotype (fig. 6 C and D). This was not due to the lack of stimulation of a fraction of starting Naïve-like cells because the numbers of Naïve-like cells were slightly yet effectively increased as compared to the input (fig. 6 E). Therefore, the Naïve-like A2/NS4b+ CD8 T cells demonstrated self-renewal, in support of their stemness potential.

In addition, we assessed Naïve-like or Non-Naïve A2/NS4b+ CD8 T cells for short-term functional readouts, in comparison to the reference subsets in Total CD8 T cells, using polyclonal anti-CD3 and anti-CD28 stimulation. First, we analyzed the proliferative marker Ki67 and the activation marker HLA-DR as early as possible i.e. at 24h, in order to avoid substantial changes in subset composition, as it naturally occurs within the first days of T cell activation *(26)*. As previously shown using isolated subsets from non-human primates *(24)*, the Total Tscm subset showed highest Ki67 expression amongst all subsets, and only Naïve cells did not upregulate HLA-DR (fig. 6 F and S5 F). Intriguingly, within A2/NS4b+ CD8 T cells, the Naïve-like population behaved similarly to the reference Total Naïve, while Non-Naïve A2/NS4b+ cells were comparable to Total EM and EMRA subsets. (fig. 6 F). Secretion of IFNγ, TNFα and IL-2 was also assessed at 4h after anti-CD3 and anti-CD28 stimulation. However, the medium control showed substantial background secretion in A2/NS4b+ populations, which could be due to activation by the tetramer staining (unavoidable for the experiment). This technical limitation precluded conclusions when

384 comparing A2/NS4b+ to the reference subsets in total CD8 T cells (not stained with
385 tetramer) (fig. S6).
386
387 Overall, these short-term functional assays showed that the behavior of Naïve-like
388 A2/NS4b+ CD8 T cells was close to the reference Total Naïve subset, in agreement with
389 their high degree of "Naïveness" observed in the whole transcriptome analyses described
390 in fig. 5.

Discussion

In this study, we report two major findings that provide new insights into the biology of long-term persisting human memory CD8 T cells. First, the YF-17D vaccine induced a population of Naïve-like memory CD8 T cells that resembles the recently described Tscm subset and preserves a high degree of "Naïveness". This was detected in a controlled setting, that is, in an antigen-specific setting with a known time of antigen priming in humans. Second, the A2/NS4b+ Naïve-like population appeared stable over at least 25 years of vaccination history. This setting provided proof for the longevity and stability of CD8 Tscm in humans, being in the range of decades.

Several studies have previously analyzed the frequencies and differentiation status of YF vaccine-induced CD8 T cells early following vaccination. These include consideration of several epitopes up to 90 days post-vaccination *(16)*, analyses on various differentiation markers mostly within the first 90 days and with limited numbers of donors up to 27 months *(13)* as well as describing the TCR repertoire in two donors up to 54 months post-vaccination *(20)*. Overall, these studies found a predominant EMRA population that is highly polyfunctional, which is unexpected for EMRA cells as they are normally considered to be terminally differentiated *(10)*. Of note, similar observations were made in CD8 T cells induced by the Smallpox vaccine, a second live-attenuated vaccine that triggers very effective CD8 T cells in humans *(10, 15)*.

Relevant to our findings, the flow cytometry data presented in these previous reports also shows evidence for a CD45RA+ CCR7+ double positive population in YF-specific CD8 T cells, either within the first 90 days (n=up to 15) *(13, 16)* or in limited numbers of donors

up to 46 months (n= 1 to 3) post-vaccination *(13, 20)*. This would correspond to the Naïve-like A2/NS4b+ CD8 T cells that we hereby report. However, this detection of Naïve-like memory CD8 T cells was neglected amidst the focus on the effector populations raised by the vaccine. Our study analyzed A2/NS4b+ CD8 T cells both beyond 5 years after vaccination and in a considerably large cohort (n >20). We thoroughly characterized this Naïve-like subset raised by the YF vaccine, and discovered that it resembles Tscm and becomes particularly predominant in the long-term (range of decades).

The phenotypic observation that A2/NS4b+ CD8 T cells from vaccinees falling in the conventional Naïve gate can express varying levels of CD45RA and CCR7 remains intriguing. Interestingly, the A2/NS4b+ Naïve^{high} population only increased by 1.5-fold in frequency between detectable unvaccinated controls and vaccinees. Yet, there was a clear change in phenotype, from genuine Naïve (CD58- CD95-) in unvaccinated controls to Tscm (CD58+ CD95+) in vaccinees. This particular phenotypic shift and the threshold of tetramer staining used (0.01% and >20 events, i.e. considerably high) supports that the cells analyzed were not merely background. Background events would have shown a distribution of subsets close to the total population of cells. Regarding the various populations characterized, our study is primarily descriptive of the phenotypic observations that can be made in the study of YF-specific CD8 T cells in vaccinees, and in relation to the memory subsets that have been described. In table 1, we summarize the populations that are referred to in this study, including conventional subsets in total CD8 T cells, the recently reported Tscm subset, and the A2/NS4b+ populations that we characterized in unvacccinated individuals and vaccinees. The fact that Tscm populations (whether the reference Total Tscm, or the Naïve-like A2/NS4b+ CD8 T cells) are found

within the conventional Naïve gate raises concerns on our current definition of memory subsets and Naïve cells, popularly defined by CCR7 and CD45RA *(6)*.

Out of all memory subsets, Tscm are thought to have retained the most "stemness", to be closest to the Naïve cells, and thus represent a subset of utmost interest for long-term immunity *(4, 24, 36)*. In the framework of adoptive T cell therapy, the least differentiated memory cells are thought to be the best source to generate a progeny of potent anti-tumor CD8 T cells and self-renew for long-term therapeutic efficacy *(4, 24, 37-39)*. Recently, serial adoptive transfers of single CD62L+ CM cells in mice demonstrated better stemness as opposed to more differentiated EM cells, by reconstituting immunocompetence against infection with *listeria monocytogenes (40)*. In humans and non-human primates, the quantity and quality of the progeny of the various subsets has been assessed by proliferation assays *in vitro*. It has been found that in particular Naïve cells and Tscm can self-renew and reconstitute the other differentiated populations (including Tscm when starting with Naïve) *(23, 24)*. In fact, Naïve cells represent the mature T cell type that is ready to encounter antigen with the highest stemness and pluripotency, potentially producing all types of effector and memory progenies *(36, 37, 41)*. Yet Naïve cells remain to be optimally primed to respond to their cognate antigen, and adoptive T cell transfers rely on the isolation and amplification of T cells, which inevitably induces differentiation. There is thus a quest to optimally prime and minimally differentiate T cells, to generate memory cells that preserve highest proximity to Naïve and thus immunotherapeutic potential. Intriguingly, from our genome-wide mRNA profiling data, there is no apparent set of genes or a signature that minimally and significantly defines the A2/NS4b+ Naïve-like CD8 T cells. In fact, very few genes were significantly differentially expressed between Naïve, CM, Tscm or the A2/NA4b+ Naïve-like CD8 T cells. Rather, the analyses across samples highlighted a

differentiation gradient defined globally by contributions from several genes, transitioning from Naïve to A2/SN4b+ Naïve-like to a mixture of Tscm/CM to Effectors. This supports the notion that CD8 T cells undergo differentiation programs upon priming, within which memory cells may retain varying proximity to the Naïve cells. In the course of an immune response, memory precursors that are rescued at the earliest differentiation stage would generate memory populations that preserve higher stemness and multipotency *(36, 42)*. Thus, the proximity to the Naïve cells, that is, the "Naïveness" of a memory cell may be regarded as the parameter that reflects early rescue and may therefore serve as a measure of memory quality. In this regard, "Naïveness" is beyond the property of stemness and reflects globally the preservation of Naïve properties. Overall, we found that Naïve-like A2/NS4b+ CD8 T cells: i) phenotypically resembled the Tscm subset by expressing markers such as CD58, CD95, CXCR3, IL-2Rβ and high LFA-1 *(23)*, ii) efficiently responded to cognate peptide and IL-15-driven homeostatic proliferation, in contrast to genuine Naïve cells; and iii) showed self-renewal capacity. Yet A2/NS4b+ Naïve-like CD8 T were not identical to the reference Total Tscm and also shared certain behaviors with the reference Naïve subset, as observed in the genome-wide transcriptome profile and short-term functional characteristics (early Ki67 and HLA-DR upregulation upon activation). In fact, in the latter analyses, the Total Tscm were very close to Total CM. Altogether, it is possible that there is substantial variation in the quality of various antigen-specific Tscm cells (and memory subsets in general), with different histories of priming and antigen exposure that may impact on phenotype and functionality. The high degree of "Naïveness" of YF-specific CD8 T cells may reflect absence of chronic or recent antigen exposure, as opposed to the Total Tscm subset that may contain variably and possibly relatively recently activated cells. This high "Naïveness" also suggests that Naïve-like A2/NS4b+ CD8 T cells are a particularly high quality population within the Tscm subset.

As addressed in the results section, the Tscm subset described by Gattinoni et al. has also been detected in the context of cancer or viral specificities, namely Melan-A, CMV and Flu *(23)*. We also detected Naïve-like CD8 T cells in CMV-, EBV- and Flu-specific CD8 T cells albeit with variation in the expression of Tscm markers such as CD58, CXCR3 and CD95. Yet the key point in our study is that the exposure to Flu, CMV and EBV viruses is difficult to track and supervise experimentally, given the chronic and/or prevalent quality of these viral infections in the human population. This contrasts to the vaccination setting, such as with YF-17D, where the parameter 'time since antigen priming' is known. The latter is the central feature to demonstrate the longevity of the vaccine-induced Naïve-like memory subset that we hereby report.

Only a few studies so far have provided proof for persistence of CD8 T cells of known antigen-specificity in the long-term, in the range of years to decades. For instance, these concern detection of CD8 and CD4 T cell responses to Poliomavirus in vaccinated individuals over two decades *(43)* and the detection of Measles-specific CD8 T cells up to 34 years after vaccination *(44)*, but no phenotypic characterization was performed. A very recently published study has gathered evidence that Tscm cells may survive at least 12 years in humans, based on the follow-up of T cell clones in cohorts of patients treated against inherited adenosine deaminase immunodeficiency with genetically corrected-hematopoietic stem cells or peripheral blood leukocytes *(45)*. Within our cohort of vaccinees, the A2/NS4b+ Naïve-like CD8 T cells were detectable for at least 25 years. The in-depth analyses showed that A2/NS4b+ Naïve-like CD8 T cells maintained higher levels of the eight markers (CD58, CD95, CXCR3, KLRG1, CD11a^{high}, IL-18Rα, Granzyme A, IL-2Rβ) that prominently distinguished them from Total Naïve, over the 17 years after vaccination studied. Moreover, we did not observe a particular correlation between expansion *in vitro*

and the vaccination history. These points altogether suggest that the qualities of the Naïve-like A2/NS4b+ CD8 T cells become apparent early after vaccination (the minimum vaccination history studied was 0.27 years) and remain relatively stable over the years-to-decades after vaccination.

Our study was confronted with two major limitations. First, the study of antigen-specific CD8 T cells is technically difficult due to their low frequencies in blood, which impose the requirement of large quantities of cells per analysis. For instance, isolation of 1'000 Naïve-like A2/NS4b+ CD8 T cells (e.g. samples for microarrays) required 100 to 500 x 10e6 PBMC, depending on the donor. A standard blood donation yields 400-1000 x10e6 PBMC, and a leukapheresis-based donation (one cycle) yields 2'000 to 8'000 x 10e6 PBMC. For an experiment using e.g. 4 samples of 1'000 purified A2/NS4b+ CD8 T cells, this would easily require the use and processing of a full blood donation.

A second limitation was the fact that the study is not longitudinal, and we need to consider the confounding variable of inter-donor variability. Only longitudinal studies may comprehend the development and stability of this A2/NS4b+ CD8 Tscm population during YF vaccination, including the clonotypic composition, expansion and inter-relations amongst subsets, and the reaction upon administration of a recall vaccine. The diversity of YF epitopes across vaccinees and the high prevalence A2/NS4b+ CD8 T cells in HLA-A*02 positive donors (fig. S3, *(13, 14)*) raise questions on the immunodominance of YF epitopes, whether host-related characteristics (e.g. HLA allele) influence the outcome of the immune response and long-term memory elicited by the YF vaccine; and whether there are links to side-effects or the efficacy of protection to infection. In view of the results of our screen on CD8 T cell YF specificities other than A2/NS4b, very large number of donors (beyond the size of our cohort) would be necessary to accumulate positive samples for the various HLA

restrictions and epitopes. In agreement with previous studies *(13, 14)*, our tetramer screen illustrated the high prevalence of the A2/NS4b specificity (LLWNGPMAV) and thus its practicality as a model antigen in humans. Nonetheless, our study has the practical advantage of avoiding the awaiting of decades to study cohorts of vaccinees with very long vaccination times. Altogether, our results support that YF vaccination is particularly suitable to investigate innate and specific immune mechanisms responsible for the generation and maintenance of self-renewing and very long-lasting memory cells in humans.

Materials and Methods

Study design, population and ethics statement

The study was open to healthy volunteers aged 18 to 65 years having received the Yellow Fever 17D vaccine (Stamaril®, Sanofi Pasteur Pty Ltd) with no limit on minimum or maximum vaccination history. Vaccinees were grouped according to years since vaccination: <1 year (I), 1-5 years (II), 5-10 years (III) and >10 years (IV). The targeted sample size was n=10 per group, and this was met for all groups except group I. No outliers were excluded from analyses. The study protocol was approved by the Human Research Ethics Committee of the Canton de Vaud (protocol 329/12), with healthy volunteers participating under written informed consent. Eligible volunteers donated blood according to the standards of the Blood Transfusion Center in Epalinges, Switzerland (Service Vaudois de Transfusion Sanguine), and the leukocyte-rich fraction (buffy coat) was recovered for the study. For further in-depth analyses requiring larger number of cells, some of the volunteers (amongst those aged up to 50 years) were also invited for a leukapheresis-based donation. Samples from unvaccinated blood donors were also obtained from the Blood Transfusion Center in Epalinges.

Peripheral blood collection and preparation.

Peripheral blood mononuclear cells (PBMC) were obtained from leukocyte-rich blood samples following density gradient fractionation using Lymphoprep™. All samples were immediately cryopreserved in RPMI 1640 supplemented with 40% FCS and 10% DMSO

awaiting experimental use.

Flow cytometry.

The tetramers and antibodies used are detailed in Table S4. For the analysis of antigen-specific populations, CD8 T cells were first enriched from cryopreserved samples using the human CD8 T cell enrichment kit from StemCell™ Technologies (negative selection, per manufacturer's instructions). Stainings were performed using PBS with 5mM EDTA, 0.2% BSA and 0.2% Na-azide (FACS buffer). Tetramer stainings were performed for 40 min at RT. Surface antibody staining was then performed, followed by staining with the fixable dead-cell marker Vivid-Aqua (Molecular Probes®, Invitrogen), each step at 4°C for 30 min. Cells were fixed overnight in 1% formaldehyde (supplemented with 2% glucose and 5mM Na-azide). Intracellular staining was performed last, using antibodies in FACS buffer with 0.1% saponin for 30 min at 4°C. For Ki-67 intracellular / nuclear staining, the fixation and permeabilization was performed using the reagents from the Foxp3 staining kit from eBioscience. Samples were acquired using a Gallios flow cytometer (Beckman Coulter, 3-laser configuration), with antibody panels limited to 10-colors. The data was processed with FlowJo (Tree Star Inc., v9.5.2). Samples with antigen-specific populations below 0.01% tetramer positive cells in Total CD8 T cells were considered negative. Populations consisting of less than 20 events were not considered eligible for further analysis (e.g. no analysis of markers on non-naïve populations of A2/NS4b+ CD8 T cells in unvaccinated individuals). Isolation of cells for microarray analyses (described further below) was performed using the a BD FACSAria I flow cytometer.

Whole transcriptome microarrays: mRNA sample preparation and analysis

CD8 T cells were enriched from cryopreserved PBMC using the negative enrichment kit from StemCell™. For the flow cytometry-based purification, samples were stained with A2/NS4b-PE tetramer for 40 min, followed by surface staining for 30 min (CD8, CD45RA, CCR7, CD16, CD58, CD95; referenced above) and live/dead staining for 30 min. For mRNA analysis on whole transcriptome, 1'000 cells were isolated from each of the five different populations using the strategy shown in fig. S6, per donor (n=8 donors, D1 to D8 ordered with increasing vaccination history), by flow cytometry-based purification directly into 13.5 ul of SumperAmp™ lysis buffer (Miltenyi Biotec). From CD8 T enrichment, all manipulations including cell sorting were carried at 4°C. After sorting, RNA lysates were incubated for 10 min at 45°C and immediately frozen at -20°C. Purifications were performed on two separate days (Sort I: D1, D3, D4 & D6; Sort II: D2, D5, D7 and D7). Thereafter, frozen RNA samples were shipped, processed and analyzed together by the Genomic Services of Miltenyi Biotec according to their SuperAmp™ technology, and by hybridization onto Agilent Whole Human Genome Microarray 8x60K (V2, one color: Cy3). The integrity of cDNA was checked via the Agilent 2100 Bioanalyzer. Fluorescence signals of the hybridized Agilent Microarrays were detected using Agilent's Microarray Scanner System (Agilent Technologies). Raw output data were generated via the Agilent Feature Extraction software. The raw data was background corrected and quantile normalized using the *backgroundCorrect* and *normalizeBetweenArrays* functions in the *limma* R package (version 3.20.8, R version 3.1.0). Control probes and probes whose normalized expression value did not exceed the background level in any of the samples were filtered out, and the expression of replicated probes were averaged, leaving 41,923 probes that were used for further analysis. Exploratory principal component analysis was performed

with the *prcomp* function in R. Since the differences between the cell populations were supposed to affect only a relatively small subset of the genes, an independent filtering procedure was applied to exclude the probes with the lowest variance across all samples, keeping only the 10% most variable probes. All probes were standardized by subtracting the mean value and dividing by the standard deviation across all samples before applying the PCA. We extracted the top 50 probes with positive and negative loadings, respectively, on the first principal component and constructed a heatmap of their expression levels across the samples (fig. 5C). To further illustrate the similarities between samples from the different cell populations, we calculated the Euclidean distance between all pairs of samples along the first principal component. The distributions of pairwise distances between samples from each pair of distinct subgroups, as well as pairwise distances between samples within each subgroup, are summarized with boxplots in fig. 5D ("inter-sample distances"). Differential expression analysis was performed with the *limma* R package (version 3.20.8). For each pair of cell populations, we performed a gene-wise moderated paired t-test, accounting for inter-donor differences. The nominal p-values were adjusted for multiple comparisons using the Benjamini-Hochberg procedure *(46)*. Hierarchical clustering was performed using Euclidean distance and complete linkage.

Proliferation assays and *in vitro* stimulations.

The Complete Medium used was RPMI 1640, complemented with 10% heat-inactivated FCS, 1% non-essential aminoacids (Gibco), 1% L-glutamine (Gibco), Hepes (10mM) and 10'000 U/ml of penicillin/streptomycin (Gibco). For the proliferation assays using NS4b peptide and cytokines, PBMC were thawed and cultured at 1.0-1.5 x 10^6 cells per ml per

649 2cm^2 in flat-bottom plates, using NS4b$^{214-222}$ peptide (LLWNGPMAV) at 1 ug/ml, human IL-
650 2 at 100 U/ml (Proleukin®, Roche Pharma) and recombinant human IL-15 at 20 U/ml (10
651 ng/ml, Peprotech). For the quantification of proliferation, the 'input (counts at start)' of
652 A2/NS4b+ CD8 T cells was calculated based on the number of PBMC seeded and the % of
653 A2/NS4b+ CD8 T cells determined by flow cytometry. The 'counts at day 7' were quantified
654 based on absolute numbers of A2/NS4b+ CD8 T cells upon full acquisition of samples by
655 flow cytometry. The 'expansion' was calculated dividing the 'counts at day 7' by the 'input'.
656 For the expansion of purified Naïve-like or Non-Naïve YF-specific CD8 T cells, A2/NS4b+
657 CD8 T cells were isolated by flow cytometry cell sorting (same strategy as the samples used
658 for whole transcriptome analyses). 200 to 4'000 cells (depending on the donor's respective
659 frequencies of A2/NS4b+ and subsequent Naïve-like/Non-Naïve phenotype) were isolated
660 and stimulated in U-bottom 96-well plates with 1ug /ml PHA, 150 U/ml IL-2 and 10e6/ ml
661 "feeder" cells. These "feeders" were prepared by mixing freshly prepared PBMC from two
662 independent blood donors, irradiated with 30Gy. The medium composition was the same
663 as above, except human serum was used instead of FCS. Medium was renewed and cells
664 were split periodically until sufficient cells had expanded to allow analysis (cell counting to
665 assess population doubling and flow cytometry), i.e. at day 14. For the experiments using
666 anti-CD3 and anti-CD28 stimulation to assess short-term function, PBMC were first thawed
667 and rested overnight in complete medium (in absence of cytokines) at a density of 0.75-1 x
668 10^6 cells per cm^2 per 0.5ml. Next day, CD8 T cells were enriched using the negative
669 selection kit from StemCell™ Technologies (per manufacturer's instructions). Importantly,
670 CD8 T cells were stained with A2/NS4b APC tetramer before as well as after the
671 stimulation with beads, in order minimize the loss of detection of tetramer positive cells
672 due to the TCR internalization that inherently occurs upon T cell activation; of note, this
673 phenomenon impacts on the quality of the tetramer staining following T cell stimulation

and renders the population of tetramer positive cells less distinct as opposed to *ex-vivo* analyses (fig. S5 F and S5 A: activated, *versus* fig. 1A: ex-vivo). Tetramer-stained CD8 T cells were plated at $2.5x10^6$ cells per 2.5 ml per $4cm^2$ (12-well plate), per condition and stimulated with anti-CD3 and anti-CD28 beads (Miltenyi Biotec) at a 1:1 ratio. For the intracellular cytokine readout at 4h, Brefeldin A was added at 10ug/ml (no cytokines). For the readout at 24h, the medium was supplemented with 100 U/ml IL-2.

Quantifications and statistical analysis.

Quantifications were made based on the softwares FlowJo, Microsoft Excel, Graphpad Prism and SPICE softwares. Statistical values were obtained using the analyses and tests (including normality tests) as detailed in the figure legends; where indicated, *ns* = not significant; * = p <0.05; ** = p <0.01; *** = p <0.001. For statistical comparison of pie charts generated using SPICE, the built-in test in SPICE software (v5.3) was used (using 10'000 permutations) *(47)*.

List of Supplementary Materials:

Fig. S1. Influence of inter-donor and age-related variability and its normalization for the study of A2/NS4b+ CD8 T cell subsets.

Fig. S2. Data complementary to fig. 3.

Fig. S3. Analyses of CD8 T cells specific for Yellow Fever epitopes alternative to the HLA-A*02-restricted NS4b.

Fig. S4. Data complementary to fig. 5.

Fig. S5. Data complementary to fig. 6.

699 Fig. S6. Cytokine production by NS4b-specific CD8 T cell subsets in comparison the
700 reference subsets in Total CD8 T cells.
701 Table S2. Main genes contributing to PC1.
702 Table S3. Differentially expressed genes comparing Naïve-like A2/NS4b+ CD8 T cells to
703 the other four subsets listed
704 Table S4: Tetramers and antibodies used for Flow Cytometry analyses.

References:

1. N. Zhang, M. J. Bevan, CD8+ T Cells: Foot Soldiers of the Immune System, *Immunity* **35**, 161–168 (2011).

2. W. H. Fridman, F. Pagès, C. Sautès-Fridman, J. Galon, The immune contexture in human tumours: impact on clinical outcome, *Nature Publishing Group* **12**, 298–306 (2012).

3. N. P. Restifo, M. E. Dudley, S. A. Rosenberg, Adoptive immunotherapy for cancer: harnessing the T cell response, *Nat Rev Immunol* **12**, 269–281 (2012).

4. L. Gattinoni, C. A. Klebanoff, N. P. Restifo, Paths to stemness: building the ultimate antitumour T cell, *Nat Rev Cancer* **12**, 671–684 (2012).

5. M. Zanetti, S. P. Schoenberger, Memory T Cells. Preface, *Adv. Exp. Med. Biol.* **684**, vii–ix (2010).

6. V. Appay, R. A. W. van Lier, F. Sallusto, M. Roederer, Phenotype and function of human T lymphocyte subsets: consensus and issues, *Cytometry A* **73**, 975–983 (2008).

7. J. R. Currier, E. G. Kuta, E. Turk, L. B. Earhart, L. Loomis-Price, S. Janetzki, G. Ferrari, D. L. Birx, J. H. Cox, A panel of MHC class I restricted viral peptides for use as a quality control for vaccine trial ELISPOT assays, *Journal of Immunological Methods* **260**, 157–172 (2002).

8. B. Pulendran, J. Z. Oh, H. I. Nakaya, R. Ravindran, D. A. Kazmin, Immunity to viruses: learning from successful human vaccines, *Immunological Reviews* **255**, 243–255 (2013).

9. S. A. Plotkin, Vaccines: correlates of vaccine-induced immunity, *Clin. Infect. Dis.* **47**, 401–409 (2008).

10. R. Ahmed, R. S. Akondy, Insights into human CD8+ T-cell memory using the yellow fever and smallpox vaccines, *Immunology and Cell Biology* **89**, 340–345 (2011).

11. B. Pulendran, Learning immunology from the yellow fever vaccine: innate immunity to systems vaccinology, *Nat Rev Immunol* **9**, 741–747 (2009).

12. M. Niedrig, M. Lademann, P. Emmerich, M. Lafrenz, Assessment of IgG antibodies against yellow fever virus after vaccination with 17D by different assays: neutralization test, haemagglutination inhibition test, immunofluorescence assay and ELISA, *Trop. Med. Int. Health* **4**, 867–871 (1999).

13. R. S. Akondy, N. D. Monson, J. D. Miller, S. Edupuganti, D. Teuwen, H. Wu, F. Quyyumi, S. Garg, J. D. Altman, C. Del Rio, H. L. Keyserling, A. Ploss, C. M. Rice, W. A. Orenstein, M. J. Mulligan, R. Ahmed, The Yellow Fever Virus Vaccine Induces a Broad and Polyfunctional Human Memory CD8+ T Cell Response, *The Journal of Immunology* **183**, 7919–7930 (2009).

14. A. B. de Melo, E. J. M. Nascimento, U. Braga-Neto, R. Dhalia, A. M. Silva, M. Oelke, J. P. Schneck, J. Sidney, A. Sette, S. M. L. Montenegro, E. T. A. Marques, T-cell memory responses elicited by yellow fever vaccine are targeted to overlapping epitopes containing multiple HLA-I and -II binding motifs, *PLoS Negl Trop Dis* **7**, e1938 (2013).

15. J. D. Miller, R. G. van der Most, R. S. Akondy, J. T. Glidewell, S. Albott, D. Masopust, K. Murali-Krishna, P. L. Mahar, S. Edupuganti, S. Lalor, S. Germon, C. Del Rio, M. J. Mulligan, S. I. Staprans, J. D. Altman, M. B. Feinberg, R. Ahmed, Human effector and memory CD8+ T cell responses to smallpox and yellow fever vaccines, *Immunity* **28**, 710–722 (2008).

16. K. Blom, M. Braun, M. A. Ivarsson, V. D. Gonzalez, K. Falconer, M. Moll, H. G. Ljunggren, J. Michaelsson, J. K. Sandberg, Temporal Dynamics of the Primary Human T Cell Response to Yellow Fever Virus 17D As It Matures from an Effector- to a Memory-Type Response, *The Journal of Immunology* **190**, 2150–2158 (2013).

17. T. Querec, S. Bennouna, S. Alkan, Y. Laouar, K. Gorden, R. Flavell, S. Akira, R. Ahmed, B. Pulendran, Yellow fever vaccine YF-17D activates multiple dendritic cell subsets via TLR2, 7, 8, and 9 to stimulate polyvalent immunity, *J. Exp. Med.* **203**, 413–424 (2006).

18. T. D. Querec, R. S. Akondy, E. K. Lee, W. Cao, H. I. Nakaya, D. Teuwen, A. Pirani, K. Gernert, J. Deng, B. Marzolf, K. Kennedy, H. Wu, S. Bennouna, H. Oluoch, J. Miller, R. Z. Vencio, M. Mulligan, A. Aderem, R. Ahmed, B. Pulendran, Systems biology approach predicts immunogenicity of the yellow fever vaccine in humans, *Nature Publishing Group* **10**, 116–125 (2009).

19. D. Gaucher, R. Therrien, N. Kettaf, B. R. Angermann, G. Boucher, A. Filali-Mouhim, J. M. Moser, R. S. Mehta, D. R. Drake, E. Castro, R. Akondy, A. Rinfret, B. Yassine-Diab, E. A. Said, Y. Chouikh, M. J. Cameron, R. Clum, D. Kelvin, R. Somogyi, L. D. Greller, R. S. Balderas, P. Wilkinson, G. Pantaleo, J. Tartaglia, E. K. Haddad, R. P. Sekaly, Yellow fever vaccine induces integrated multilineage and polyfunctional immune responses, *Journal of Experimental Medicine* **205**, 3119–3131 (2008).

20. M. D. T. Co, E. D. Kilpatrick, A. L. Rothman, Dynamics of the CD8 T-cell response following yellow fever virus 17D immunization, *Immunology* **128**, e718–e727 (2009).

21. N. Rufer, T. H. Brümmendorf, S. Kolvraa, C. Bischoff, K. Christensen, L. Wadsworth, M. Schulzer, P. M. Lansdorp, Telomere fluorescence measurements in granulocytes and T lymphocyte subsets point to a high turnover of hematopoietic stem cells and memory T cells in early childhood, *J. Exp. Med.* **190**, 157–167 (1999).

22. R. Vescovini, F. F. Fagnoni, A. R. Telera, L. Bucci, M. Pedrazzoni, F. Magalini, A. Stella, F. Pasin, M. C. Medici, A. Calderaro, R. Volpi, D. Monti, C. Franceschi, J. Nikolich-Žugich, P. Sansoni, Naïve and memory CD8 T cell pool homeostasis in advanced aging: impact of age and of antigen-specific responses to cytomegalovirus, *Age (Dordr)* **36**, 625–640 (2014).

23. L. Gattinoni, E. Lugli, Y. Ji, Z. Pos, C. M. Paulos, M. F. Quigley, J. R. Almeida, E. Gostick, Z. Yu, C. Carpenito, E. Wang, D. C. Douek, D. A. Price, C. H. June, F. M. Marincola, M. Roederer, N. P. Restifo, A human memory T cell subset with stem cell–like properties, *Nature Medicine* **17**, 1290–1297 (2011).

24. E. Lugli, M. H. Dominguez, L. Gattinoni, P. K. Chattopadhyay, D. L. Bolton, K. Song, N. R. Klatt, J. M. Brenchley, M. Vaccari, E. Gostick, D. A. Price, T. A. Waldmann, N. P. Restifo, G. Franchini, M. Roederer, Superior T memory stem cell persistence supports long-lived T cell memory, *J. Clin. Invest.* (2013), doi:10.1172/JCI66327DS1.

25. E. Lugli, L. Gattinoni, A. Roberto, D. Mavilio, D. A. Price, N. P. Restifo, M. Roederer, Identification, isolation and in vitro expansion of human and nonhuman primate T stem

784 cell memory cells, *Nat Protoc* **8**, 33–42 (2012).

785 26. A. Legat, D. E. Speiser, H. Pircher, D. Zehn, S. A. Fuertes Marraco, Inhibitory Receptor
786 Expression Depends More Dominantly on Differentiation and Activation than "Exhaustion"
787 of Human CD8 T Cells, *Front Immunol* **4**, 455 (2013).

788 27. S. H. C. Havenith, S. L. Yong, S. M. Henson, B. Piet, M. M. Idu, S. D. Koch, R. E. Jonkers, N. A.
789 M. Kragten, A. N. Akbar, R. A. W. van Lier, I. J. M. Ten Berge, Analysis of stem-cell-like
790 properties of human CD161++IL-18Rα+ memory CD8+ T cells, *International Immunology*
791 **24**, 625–636 (2012).

792 28. C. J. Turtle, H. M. Swanson, N. Fujii, E. H. Estey, S. R. Riddell, A distinct subset of self-
793 renewing human memory CD8+ T cells survives cytotoxic chemotherapy, *Immunity* **31**,
794 834–844 (2009).

795 29. D. Masopust, D. Choo, V. Vezys, E. J. Wherry, J. Duraiswamy, R. Akondy, J. Wang, K. A.
796 Casey, D. L. Barber, K. S. Kawamura, K. A. Fraser, R. J. Webby, V. Brinkmann, E. C. Butcher, K.
797 A. Newell, R. Ahmed, Dynamic T cell migration program provides resident memory within
798 intestinal epithelium, *Journal of Experimental Medicine* **207**, 553–564 (2010).

799 30. J. M. Schenkel, D. Masopust, Identification of a resident T-cell memory core
800 transcriptional signature, *Immunology and Cell Biology* **92**, 8–9 (2014).

801 31. M. J. Pittet, D. Valmori, P. R. Dunbar, D. E. Speiser, D. Liénard, F. Lejeune, K. Fleischhauer,
802 V. Cerundolo, J. C. Cerottini, P. Romero, High frequencies of naive Melan-A/MART-1-specific
803 CD8(+) T cells in a large proportion of human histocompatibility leukocyte antigen (HLA)-
804 A2 individuals, *J. Exp. Med.* **190**, 705–715 (1999).

805 32. L. Baitsch, A. Legat, L. Barba, S. A. Fuertes Marraco, J.-P. Rivals, P. Baumgaertner, C.
806 Christiansen-Jucht, H. Bouzourene, D. Rimoldi, H. Pircher, N. Rufer, M. Matter, O. Michielin,
807 D. E. Speiser, H. M. Ashour, Ed. Extended Co-Expression of Inhibitory Receptors by Human
808 CD8 T-Cells Depending on Differentiation, Antigen-Specificity and Anatomical Localization,
809 *PLoS ONE* **7**, e30852 (2012).

810 33. J. T. Tan, B. Ernst, W. C. Kieper, E. LeRoy, J. Sprent, C. D. Surh, Interleukin (IL)-15 and IL-
811 7 jointly regulate homeostatic proliferation of memory phenotype CD8+ cells but are not
812 required for memory phenotype CD4+ cells, *J. Exp. Med.* **195**, 1523–1532 (2002).

813 34. J. E. TILL, E. A. MCCULLOCH, L. SIMINOVITCH, A STOCHASTIC MODEL OF STEM CELL
814 PROLIFERATION, BASED ON THE GROWTH OF SPLEEN COLONY-FORMING CELLS, *Proc.*
815 *Natl. Acad. Sci. U.S.A.* **51**, 29–36 (1964).

816 35. J. E. Dick, Stem cells: Self-renewal writ in blood, *Nature* **423**, 231–233 (2003).

817 36. N. P. Restifo, L. Gattinoni, Lineage relationship of effector and memory T cells, *Current*
818 *Opinion in Immunology* **25**, 556–563 (2013).

819 37. L. Gattinoni, D. J. Powell, S. A. Rosenberg, N. P. Restifo, Adoptive immunotherapy for
820 cancer: building on success, *Nat Rev Immunol* **6**, 383–393 (2006).

821 38. C. A. Klebanoff, L. Gattinoni, N. P. Restifo, Sorting through subsets: which T-cell
822 populations mediate highly effective adoptive immunotherapy? *J. Immunother.* **35**, 651–

660 (2012).

39. C. Stemberger, P. Graef, M. Odendahl, J. Albrecht, G. Dössinger, F. Anderl, V. R. Buchholz, G. Gasteiger, M. Schiemann, G. U. Grigoleit, F. R. Schuster, A. Borkhardt, B. Versluys, T. Tonn, E. Seifried, H. Einsele, L. Germeroth, D. H. Busch, M. Neuenhahn, Lowest numbers of primary CD8+ T cells can reconstitute protective immunity upon adoptive immunotherapy, *Blood* (2014), doi:10.1182/blood-2013-12-547349.

40. P. Graef, V. R. Buchholz, C. Stemberger, M. Flossdorf, L. Henkel, M. Schiemann, I. Drexler, T. Höfer, S. R. Riddell, D. H. Busch, Serial Transfer of Single-Cell-Derived Immunocompetence Reveals Stemness of CD8+ Central Memory T Cells, *Immunity* **41**, 116–126 (2014).

41. C. S. Hinrichs, Z. A. Borman, L. Gattinoni, Z. Yu, W. R. Burns, J. Huang, C. A. Klebanoff, L. A. Johnson, S. P. Kerkar, S. Yang, P. Muranski, D. C. Palmer, C. D. Scott, R. A. Morgan, P. F. Robbins, S. A. Rosenberg, N. P. Restifo, Human effector CD8+ T cells derived from naive rather than memory subsets possess superior traits for adoptive immunotherapy, *Blood* **117**, 808–814 (2011).

42. F. Sallusto, A. Lanzavecchia, Memory in disguise, *Nature Medicine* **17**, 1182–1183 (2011).

43. R. Wahid, M. J. Cannon, M. Chow, Virus-specific CD4+ and CD8+ cytotoxic T-cell responses and long-term T-cell memory in individuals vaccinated against polio, *Journal of Virology* **79**, 5988–5995 (2005).

44. D. Naniche, M. Garenne, C. Rae, M. Manchester, R. Buchta, S. K. Brodine, M. B. A. Oldstone, Decrease in measles virus-specific CD4 T cell memory in vaccinated subjects, *J. Infect. Dis.* **190**, 1387–1395 (2004).

45. L. Biasco, S. Scala, L. Basso Ricci, F. Dionisio, C. Baricordi, A. Calabria, S. Giannelli, N. Cieri, F. Barzaghi, R. Pajno, H. Al-Mousa, A. Scarselli, C. Cancrini, C. Bordignon, M. G. Roncarolo, E. Montini, C. Bonini, A. Aiuti, In vivo tracking of T cells in humans unveils decade-long survival and activity of genetically modified T memory stem cells, *Science Translational Medicine* **7**, 273ra13 (2015).

46. Y. Benjamini, Y. Hochberg, Controlling the False Discovery Rate: A Practical and Powerful Approach to Multiple Testing, *Journal of the Royal Statistical Society. Series B (Methodological)* **57**, 289–300 (1995).

47. M. Roederer, J. L. Nozzi, M. C. Nason, SPICE: exploration and analysis of post-cytometric complex multivariate datasets, *Cytometry A* **79**, 167–174 (2011).

Acknowledgements: We thank all blood donors for their participation, the personnel of the Blood Transfusion Center in Epalinges (Christine Thibaud for coordinating the Leukaphereses and Jocelyne Conne for the laboratory processing), Danny Labes (Flow Cytometry Facility of the Ludwig Cancer Center), and all the members of our laboratories.

Funding: Ludwig Cancer Research Center, the Cancer Vaccine Collaborative, the CRI (all N.Y., U.S.A), the Swiss Cancer League (02836-08-2011), the Swiss National Science Foundation (310030_135553, 320030_152856 and CRSII3_141879), and a grant of the Swiss State Secretariat for Education, Research and Innovation to the SIB for Service and infrastructure resources.

Author Contributions: SAFM, MA, DES conceived and designed the experiments. SAFM, LC, SAM, SW, DES elaborated the clinical protocol. SAFM, POG, MA, NM performed the experiments. SAFM, CS, POG, MA, MD, DES analyzed the data (statistical analyses: SAFM, CS, POG, MA). SAFM, CS, POG, MA, NR, DES wrote the paper. All authors revised and accepted the final version of the manuscript.

Competing interests: the authors declare that this study was conducted in absence of any potential conflict of interest.

Figure legends:

Fig. 1. A2/NS4b+ CD8 T cells persist long-term after YF vaccination, featuring a Naïve-like population. 41 vaccinees were studied, covering 0.27 to 35 years after vaccination (table S1). Unvaccinated donors (UN, n=10) were studied as controls. **A.** Representative flow cytometry plots showing A2/NS4b tetramer staining of total CD8 T cells. **B.** Frequencies of A2/NS4b+ cells within Total CD8 T in unvaccinated controls and in vaccinees, *versus* years since vaccination. Donors below 0.01% were considered negative. Symbols: ● = vaccinees (n=34); ○ = vaccinees with multiple vaccines (n=4; time since last vaccination is taken into account); ◇ = unvaccinated controls (UN, n=3/10); × = excluded donors: vaccinees (n=3/41) or UN ctrls (n=7/10). Linear regressions correspond to the single-shot vaccinees group (●), indicating R^2 (goodness of fit) and 95% confidence intervals. **C.** Gating strategy to discriminate differentiation subsets based on the conventional markers CCR7 and CD45RA, as indicated. **D**. Representative flow cytometry plots showing subsets (CCR7 vs CD45RA) in A2/NS4b+ CD8 T cells from various vaccinees. **E.** Subset distribution (%) within A2/NS4b-specific CD8 T cells across vaccinees, ordered vertically with increasing 'years since vaccination'.

Fig. 2. The Naïve-like population of A2/NS4b+ CD8 T cells induced by the Yellow Fever 17D vaccine is stable long-term. A and B. Quantification of the frequency of A2/NS4b+ cells amongst the various conventional subsets, showing Naïve, CM, EM, and EMRA (**A**) as well as Naïve^{high} and Naïve^{int} (**B**), *versus* increasing 'years since vaccination'. Symbols: ○ = vaccinees (n=34) ; ○ = vaccinees with multiple vaccines (n=4); time since last vaccination is taken into account); ◇ = unvaccinated controls (UN, n=3). Linear regressions shown correspond to the single-shot vaccinees group (●), with details on R^2 (goodness of

fit), line and 95% confidence intervals. **C**. Compilation of the slopes with standard error from the linear regressions shown in A and B; the slope reflects the trend for change in the LOG10 frequency of A2/NS4b+ cells with increasing time since vaccination.

Fig. 3. Naïve-like A2/NS4b+ CD8 T cells induced by the YF vaccine are clearly distinct from genuine Naïve cells and resemble the Tscm subset. A. Representative subset analysis (CCR7 vs CD45RA) of an unvaccinated donor, within A2/NS4b+ or Total CD8 T cells. **B.** Subset distribution in A2/NS4b+ CD8 T cells from unvaccinated controls ("UN", n=5) *versus* vaccinees ("VAC", n=16), showing mean and standard error. **C and D.** The indicated markers were compared in detectable A2/NS4b+ subsets in unvaccinated controls (n=3) or vaccinees (n=16), *versus* the reference subsets in Total CD8 T cells. Shown are representative off-set overlay histograms (C) and corresponding heat map-based quantifications of % positive cells (D) with Bonferroni adjusted p-values following 2-way ANOVA indicated for "UN" vs "VAC". **E.** Representative gating of the Tscm subset as CD58+ CD95+ within Total Naïve (CCR7+ CD45RA+) cells. **F.** Frequency of A2/NS4b+ cells within Total Tscm in vaccinees or unvaccinated controls (mean and SD); "n.d." = not detectable. **G and H.** As in C and D, for 18 markers further assessed in vaccinees (n=16), with Bonferroni adjusted p-values following 2-way ANOVA indicated per marker. Wilcoxon matched-pairs test to compare profiles "overall" are indicated at the bottom (complemented in fig. S2).

Fig. 4. Comparison of A2/NS4b+ CD8 T cells to other antigen-specificities. A. A selection of 16 vaccinees (as in fig. 3) was analyzed for various antigen-specific populations based on two combinatorial tetramer stainings, including Yellow Fever NS4b-specific (* = PE in staining I, PE & APC in staining II), EBV-specific (A2/EBV-PE in staining II), Flu-

929 specific (A2/Flu-MA APC in staining II), CMV-specific (A2/NLV- PE and –APC in staining I)
930 and the self-antigen Melan-A-specific (A2/ELA APC in staining I). Total CD8 T cells and
931 antigen-specific populations were analyzed for subset distribution (CCR7 vs CD45RA), and
932 subsets in turn for CD58, CD95 and CXCR3. One representative vaccinee (positive for CMV)
933 is shown. **B.** Frequencies of antigen-specific populations in the 16 vaccinees: only 5 donors
934 were positive for CMV-specific CD8 T cells, while all donors showed detectable levels of
935 Melan-A-specific CD8 T cells (fig. S5). **C**. Subset distribution in the various antigen-specific
936 CD8 T populations across donors (mean and standard error). **D.** Frequencies of cells
937 positive for CD58, CD95 and CXCR3, across differentiation subsets within the various
938 antigen-specificities or total CD8 T cells, as indicated.
939
940 **Fig. 5. The mRNA profiles of Naïve-like A2/NS4b+ CD8 T cells are similar to Tscm and**
941 **display highest "Naïveness".** Whole genome expression profiles were assessed on the five
942 populations shown color-coded in **A**, each purified from n=8 vaccinees (sorting strategy in
943 fig. S6). **B**. Sample distribution in the first two principal components (PC1 vs PC2) of the
944 Principal Component Analysis (PCA) considering the top 10% most variable genes. **C.**
945 Heatmap-based display of the main contributors to PC1 in the PCA considering the top 10%
946 variable genes, showing the 40 samples ordered by their coordinate on PC1. Note: the
947 corresponding genes are listed in table S2. **D and E**. Distribution of inter-sample Euclidean
948 distances along PC1 in the PCA considering the top 10% variable genes. Each boxplot
949 summarizes the pairwise distances between samples in A2/NS4b+ Naïve-like (left panel)
950 or Total Naïve (right panel) *versus* the population indicated on the vertical axis.
951
952 **Fig. 6. Functional characteristics of A2/NS4b+ CD8 T cells: responses to cognate**
953 **peptide and homeostatic IL-15, and self-renewal. A and B.** PBMC from vaccinees (n=35)

and unvaccinated controls (n=3) were stimulated with NS4b peptide and cytokines (IL-2 or IL-15) as indicated, for 7 days. A: expansion based on fold counts to start (mean and SD; Wilcoxon p-values paired per vaccinee). B: expansion *versus* the starting frequency of A2/NS4b+ CD8 T cells with a Naïve-like phenotype. Undetectable samples (<15 counts) were excluded. R = Spearman correlations. **C to E.** Purified A2/NS4b+ CD8 T cells, either Naïve-like (n=5) or Non-Naïve (n=4) were isolated from vaccinees and expanded with PHA, IL-2 and irradiated feeders for 14 days. C: gating strategy. D: frequencies of expanded cells with a Naïve-like phenotype, showing mean, SD and p-value from Mann-Whitney test. E: population doubling of Naïve-like cells. **F.** CD8 T cells from vaccinees (n=7) were stimulated with anti-CD3 and anti-CD28 beads for 24h. Naïve-like and Non-Naïve A2/NS4b+ CD8 T cells were analyzed for Ki67 and HLA-DR expression, in comparison to the reference subsets in Total CD8 T (gating shown in fig. S5 F). Shown is the mean and SD; with p-values from paired Wilcoxon tests.

Figure 1

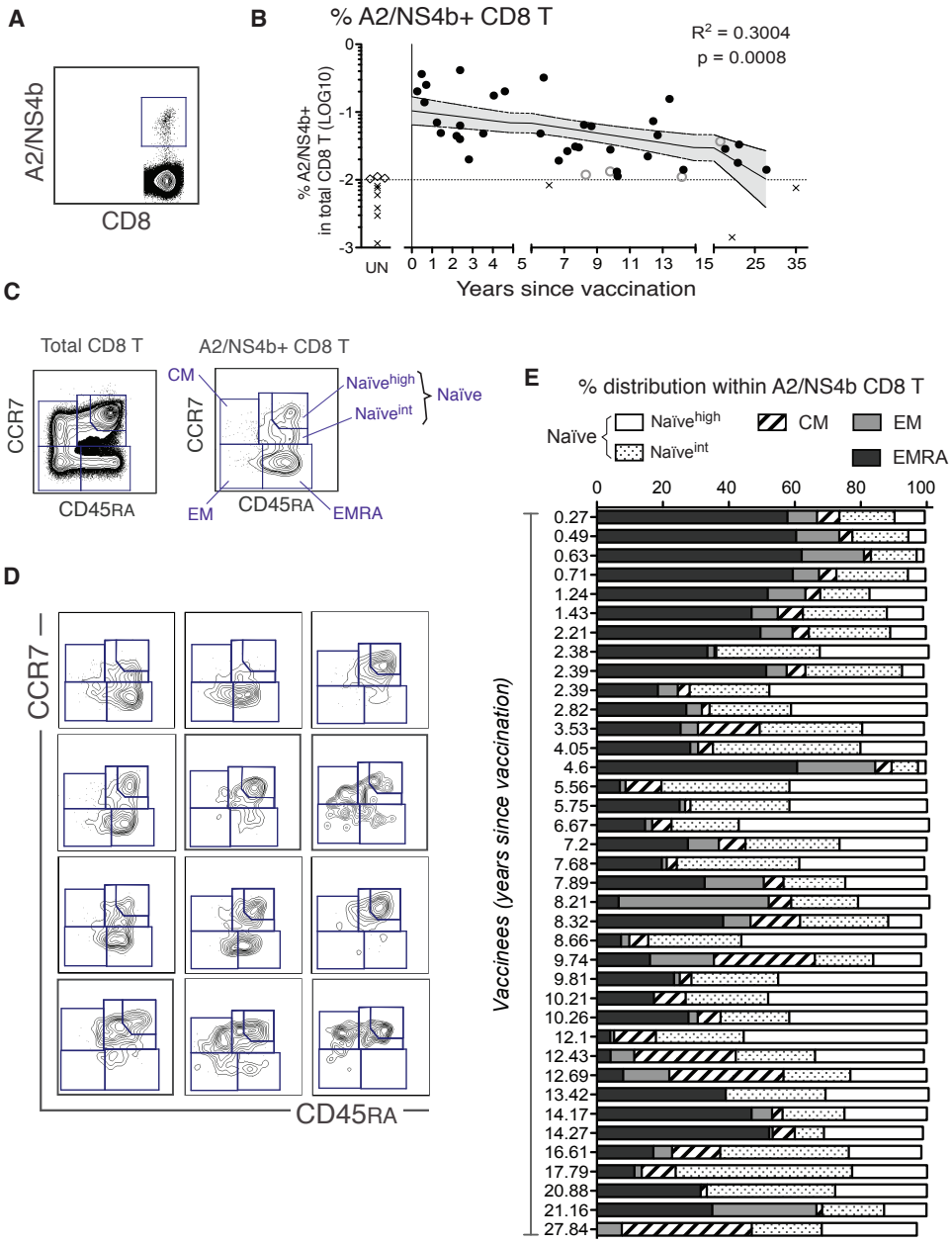
A
A2/NS4b
CD8
B
% A2/NS4b+ CD8 T
R2 = 0.3004
p = 0.0008
% A2/NS4b+ in total CD8 T (LOG10)
0
-1
-2
-3
UN
0 1 2 3 4 5 7 9 11 13 15 25 35
Years since vaccination
C
Total CD8 T
A2/NS4b+ CD8 T
CCR7
CD45RA
CM
EM
EMRA
Naïvehigh
Naïveint
Naïve
D
CCR7
CD45RA
E
% distribution within A2/NS4b CD8 T
Naïve
Naïvehigh
Naïveint
CM
EM
EMRA
0 20 40 60 80 100
Vaccinees (years since vaccination)
0.27
0.49
0.63
0.71
1.24
1.43
2.21
2.38
2.39
2.39
2.82
3.53
4.05
4.6
5.56
5.75
6.67
7.2
7.68
7.89
8.21
8.32
8.66
9.74
9.81
10.21
10.26
12.1
12.43
12.69
13.42
14.17
14.27
16.61
17.79
20.88
21.16
27.84

Figure 2

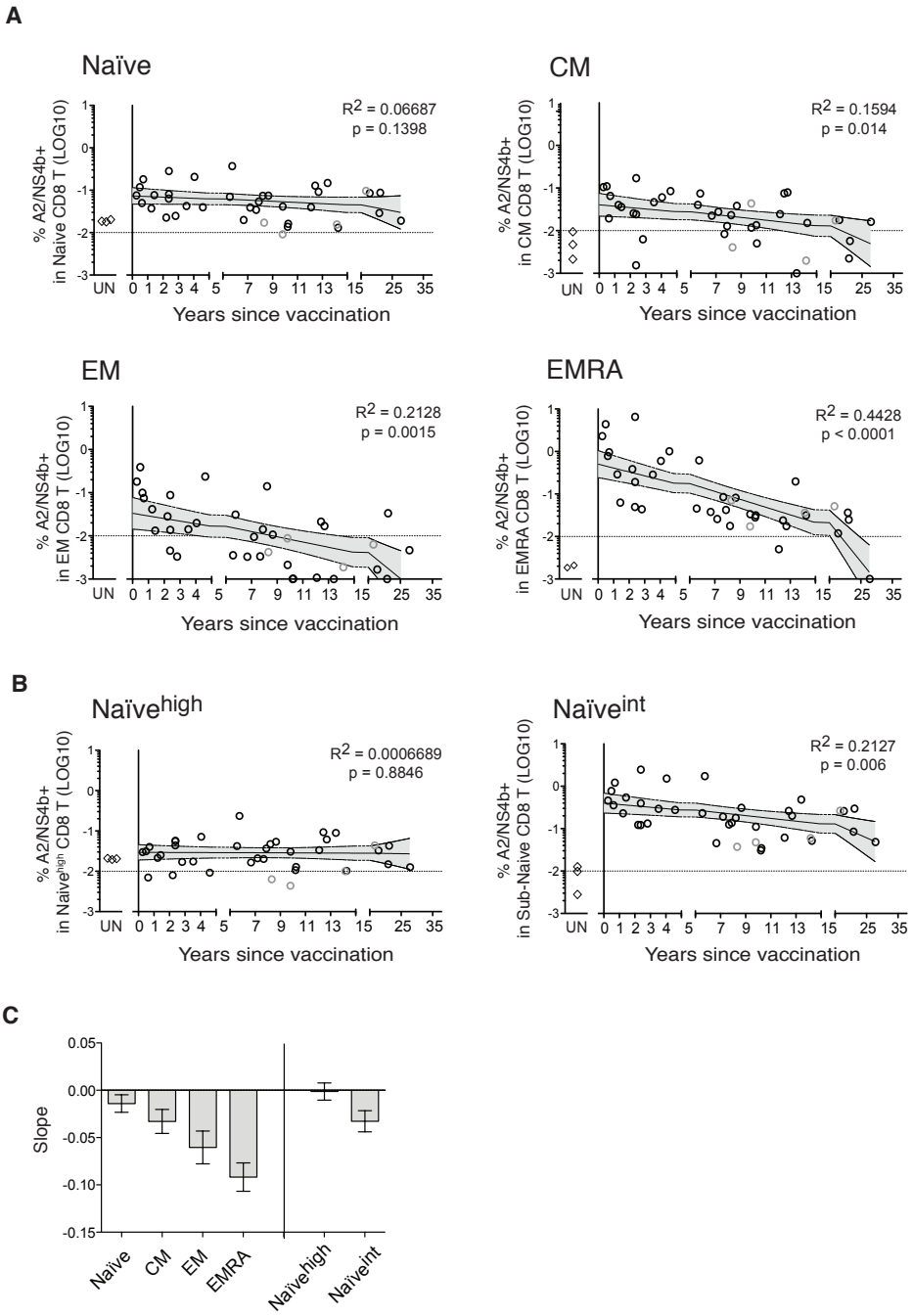
A
Naïve
R2 = 0.06687
p = 0.1398
% A2/NS4b+ in Naive CD8 T (LOG10)
CM
R2 = 0.1594
p = 0.014
% A2/NS4b+ in CM CD8 T (LOG10)
EM
R2 = 0.2128
p = 0.0015
% A2/NS4b+ in EM CD8 T (LOG10)
EMRA
R2 = 0.4428
p < 0.0001
% A2/NS4b+ in EMRA CD8 T (LOG10)
UN 0 1 2 3 4 5 7 9 11 13 15 25 35
Years since vaccination
B
Naïvehigh
R2 = 0.0006689
p = 0.8846
% A2/NS4b+ in Naivehigh CD8 T (LOG10)
Naïveint
R2 = 0.2127
p = 0.006
% A2/NS4b+ in Sub-Naive CD8 T (LOG10)
C
Slope
0.05
0.00
-0.05
-0.10
-0.15
Naïve
CM
EM
EMRA
Naïvehigh
Naïveint

Figure 3

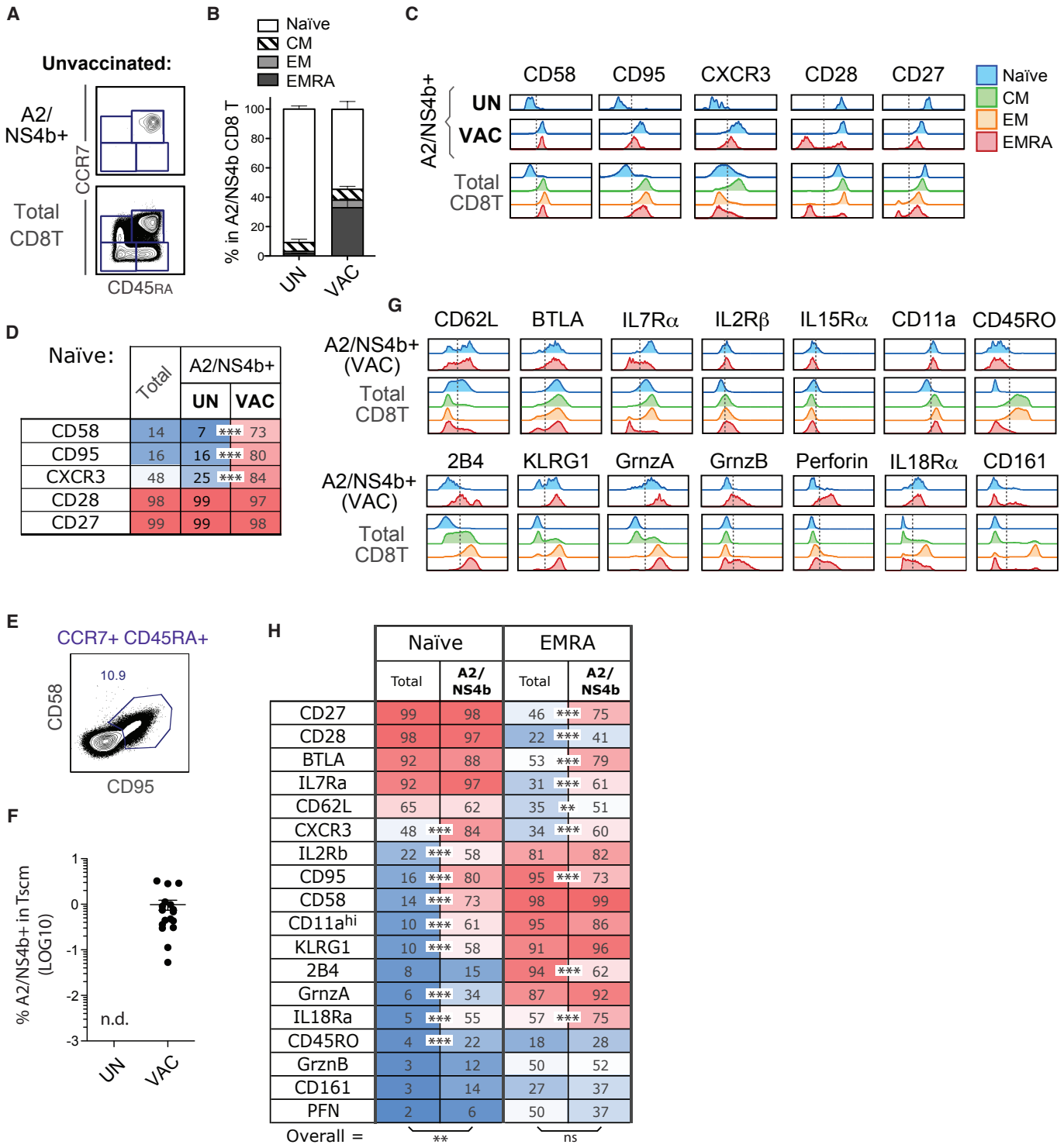
A
Unvaccinated:
A2/ NS4b+
CCR7
Total CD8T
CD45RA
B
Naïve
CM
EM
EMRA
% in A2/NS4b CD8 T
UN
VAC
C
CD58
CD95
CXCR3
CD28
CD27
A2/NS4b+
UN
VAC
Total CD8T
Naïve
CM
EM
EMRA
D
Naïve:
Total
A2/NS4b+
UN
VAC
CD58 14 7 *** 73
CD95 16 16 *** 80
CXCR3 48 25 *** 84
CD28 98 99 97
CD27 99 99 98
G
CD62L
BTLA
IL7Rα
IL2Rβ
IL15Rα
CD11a
CD45RO
A2/NS4b+ (VAC)
Total CD8T
2B4
KLRG1
GrnzA
GrnzB
Perforin
IL18Rα
CD161
E
CCR7+ CD45RA+
10.9
CD58
CD95
F
% A2/NS4b+ in Tscm (LOG10)
n.d.
UN
VAC
H
Naïve
EMRA
Total
A2/ NS4b
CD27 99 98 46 *** 75
CD28 98 97 22 *** 41
BTLA 92 88 53 *** 79
IL7Ra 92 97 31 *** 61
CD62L 65 62 35 ** 51
CXCR3 48 *** 84 34 *** 60
IL2Rb 22 *** 58 81 82
CD95 16 *** 80 95 *** 73
CD58 14 *** 73 98 99
CD11a^hi 10 *** 61 95 86
KLRG1 10 *** 58 91 96
2B4 8 15 94 *** 62
GrnzA 6 *** 34 87 92
IL18Ra 5 *** 55 57 *** 75
CD45RO 4 *** 22 18 28
GrnzB 3 12 50 52
CD161 3 14 27 37
PFN 2 6 50 37
Overall = ** ns

Figure 4

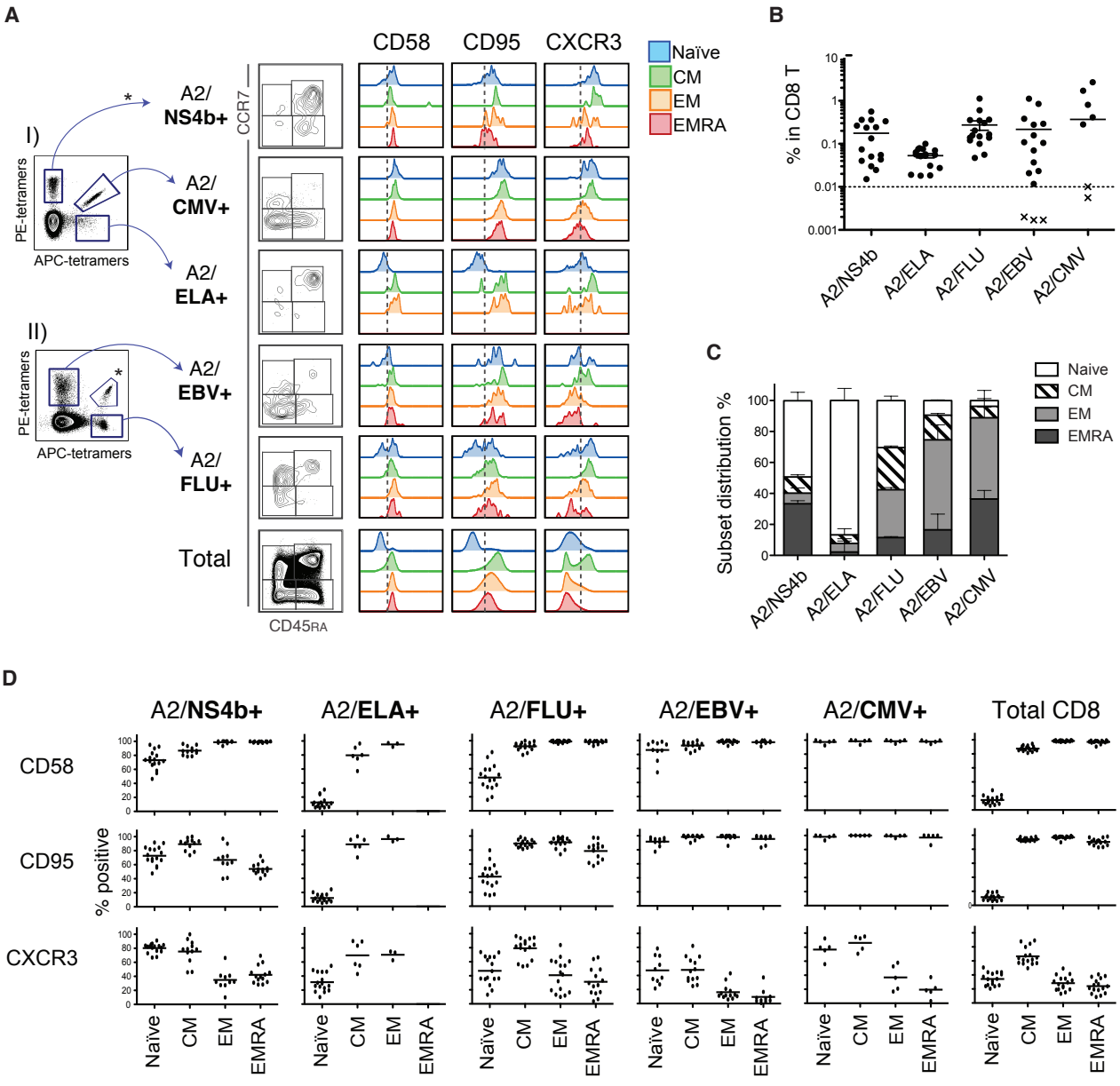
A
CD58
CD95
CXCR3
Naïve
CM
EM
EMRA
I)
PE-tetramers
APC-tetramers
A2/ NS4b+
A2/ CMV+
A2/ ELA+
II)
A2/ EBV+
A2/ FLU+
Total
CCR7
CD45RA
B
% in CD8 T
A2/NS4b
A2/ELA
A2/FLU
A2/EBV
A2/CMV
C
Subset distribution %
Naive
CM
EM
EMRA
D
A2/NS4b+
A2/ELA+
A2/FLU+
A2/EBV+
A2/CMV+
Total CD8
CD58
CD95
CXCR3
% positive
Naïve
CM
EM
EMRA

Figure 5

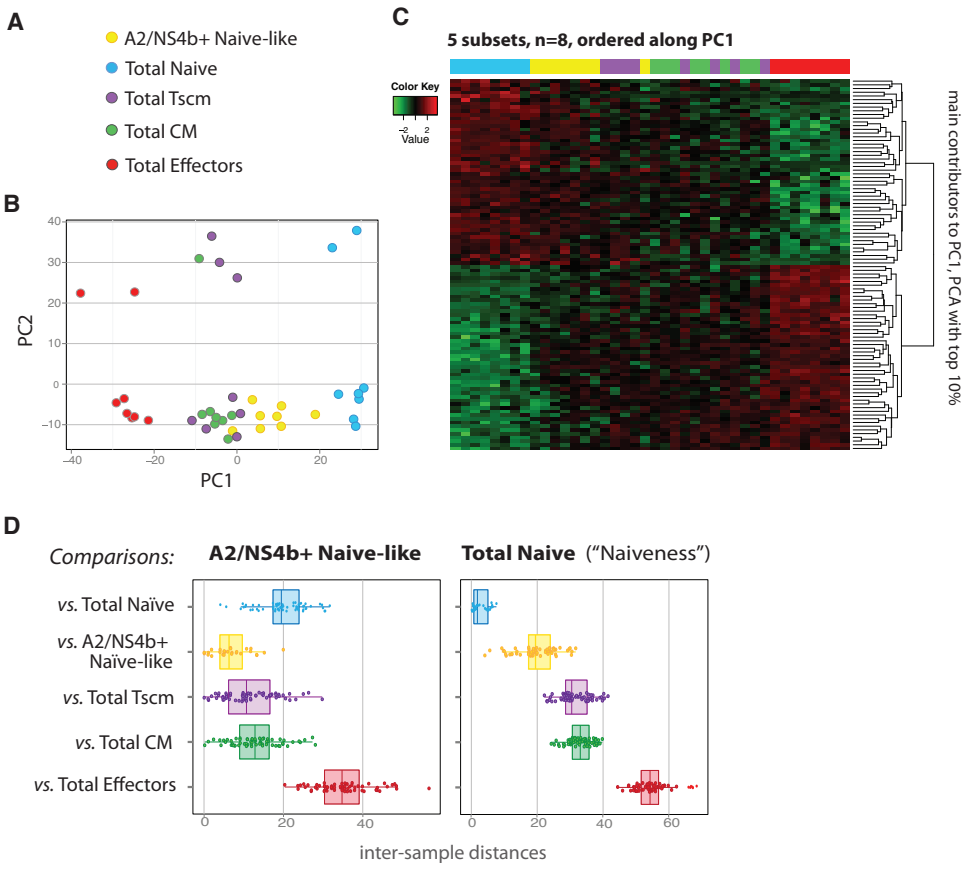
A
A2/NS4b+ Naive-like
Total Naive
Total Tscm
Total CM
Total Effectors
B
PC2
PC1
C
5 subsets, n=8, ordered along PC1
Color Key
Value
main contributors to PC1, PCA with top 10%
D
Comparisons:
A2/NS4b+ Naive-like
Total Naive ("Naiveness")
vs. Total Naïve
vs. A2/NS4b+ Naïve-like
vs. Total Tscm
vs. Total CM
vs. Total Effectors
inter-sample distances

Figure 6

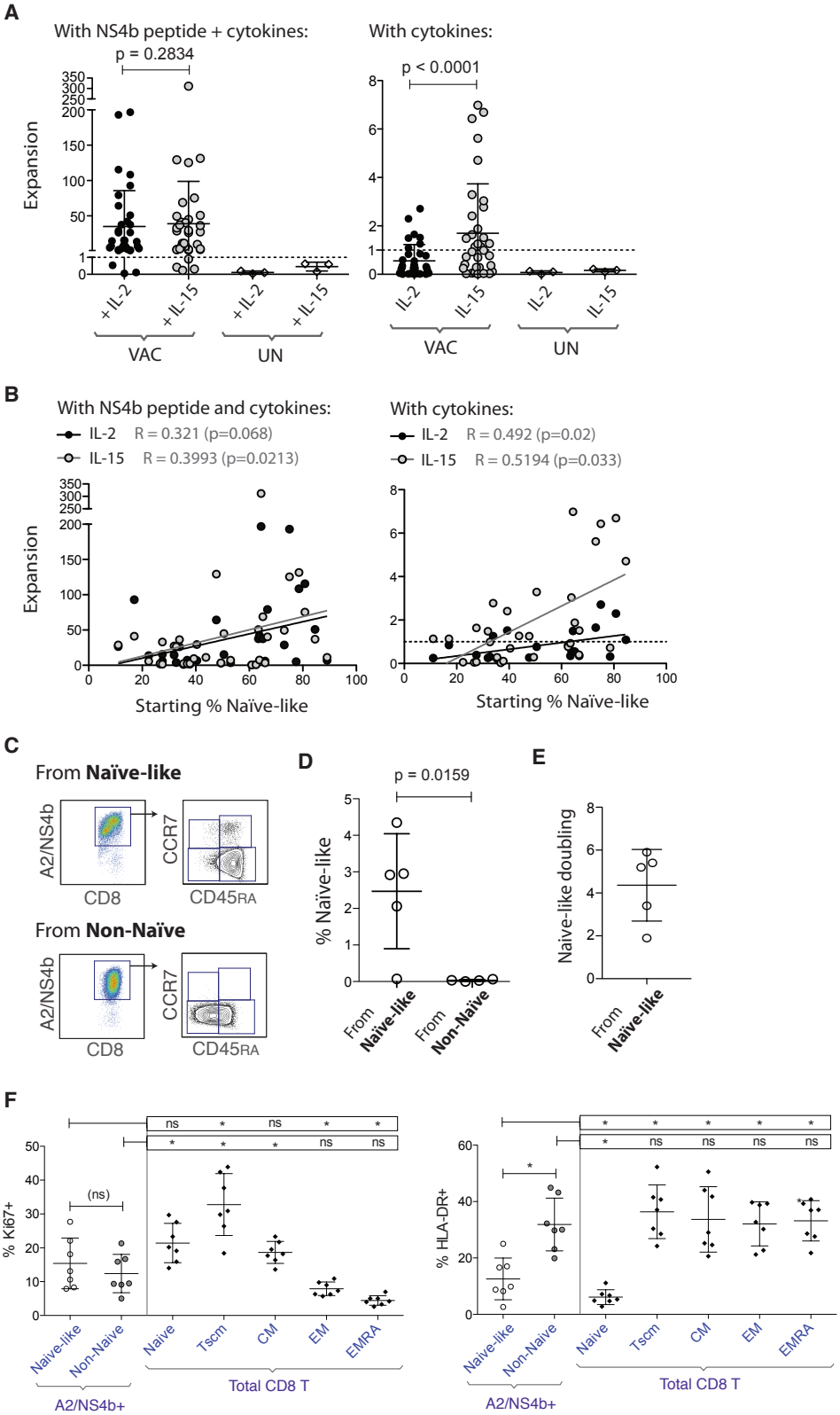
A
With NS4b peptide + cytokines:
p = 0.2834
Expansion
+IL-2
+IL-15
+IL-2
+IL-15
VAC
UN
With cytokines:
p < 0.0001
IL-2
IL-15
IL-2
IL-15
VAC
UN
B
With NS4b peptide and cytokines:
IL-2 R = 0.321 (p=0.068)
IL-15 R = 0.3993 (p=0.0213)
Expansion
Starting % Naïve-like
With cytokines:
IL-2 R = 0.492 (p=0.02)
IL-15 R = 0.5194 (p=0.033)
Starting % Naïve-like
C
From Naïve-like
A2/NS4b
CD8
CCR7
CD45RA
From Non-Naïve
A2/NS4b
CD8
CCR7
CD45RA
D
p = 0.0159
% Naïve-like
From Naïve-like
From Non-Naïve
E
Naive-like doubling
From Naïve-like
F
% Ki67+
(ns)
Naive-like
Non-Naive
Naive
Tscm
CM
EM
EMRA
A2/NS4b+
Total CD8 T
% HLA-DR+
Naive-like
Non-Naive
Naive
Tscm
CM
EM
EMRA
A2/NS4b+
Total CD8 T

969 **Table 1. Summary of the CD8 T cell populations referred to in this study.**

Population	***Subset***	***CCR7 and CD45RA** (6)*	***Additional markers:***
Total Naive	Conventional Naive (6)	CCR7+ CD45RA+ (in total CD8 T)	CD58- CD95- CD28+ CD27+
Total Tscm	Tscm; recently reported subset: "largely Naïve-like" with high levels of certain markers such as CD58 and CD95 (23-25))	CCR7+ CD45RA+ (in total CD8 T)	CD58+ CD95+ CD28+ CD27+
Total CM	Conventional CM (6)	CCR7+ CD45RA- (in total CD8 T)	CD58+ CD95+ CD28+ CD27+
Total EM	Conventional EM (6)	CCR7- CD45RA- (in total CD8 T)	CD58+ CD95+ CD28+/- CD27+
Total EMRA	Conventional EMRA (6)	CCR7- CD45RA+ (in total CD8 T)	CD58+ CD95+ CD28- CD27-
A2/NS4b+ Naive in **unvaccinated**	Naïve (no antigen experience, i.e. genuinely Naive)	CCR7+ CD45RA+	CD58- CD95- CD28+ CD27+
A2/NS4b+ Naive-like in **vaccinees**	Tscm as defined by markers; with proximity to Conventional Naïve ("Naïveness") in terms of whole transcriptome and short-term function	CCR7+ CD45RA+; can be CCR7high CD45RAhigh (Naive-high) or CCR7int CD45RAint (Naïve-int)	CD58+ CD95+ CD28+ CD27+
A2/NS4b+ EMRA in **vaccinees**	EMRA with particular differences (10, 13) such as high levels of CD28, CD27, IL7Ra, CXCR3, CD62L and BTLA	CCR7- CD45RA+	CD58+ CD95+ CD28+/- CD27+

970

971

972

Figure S1

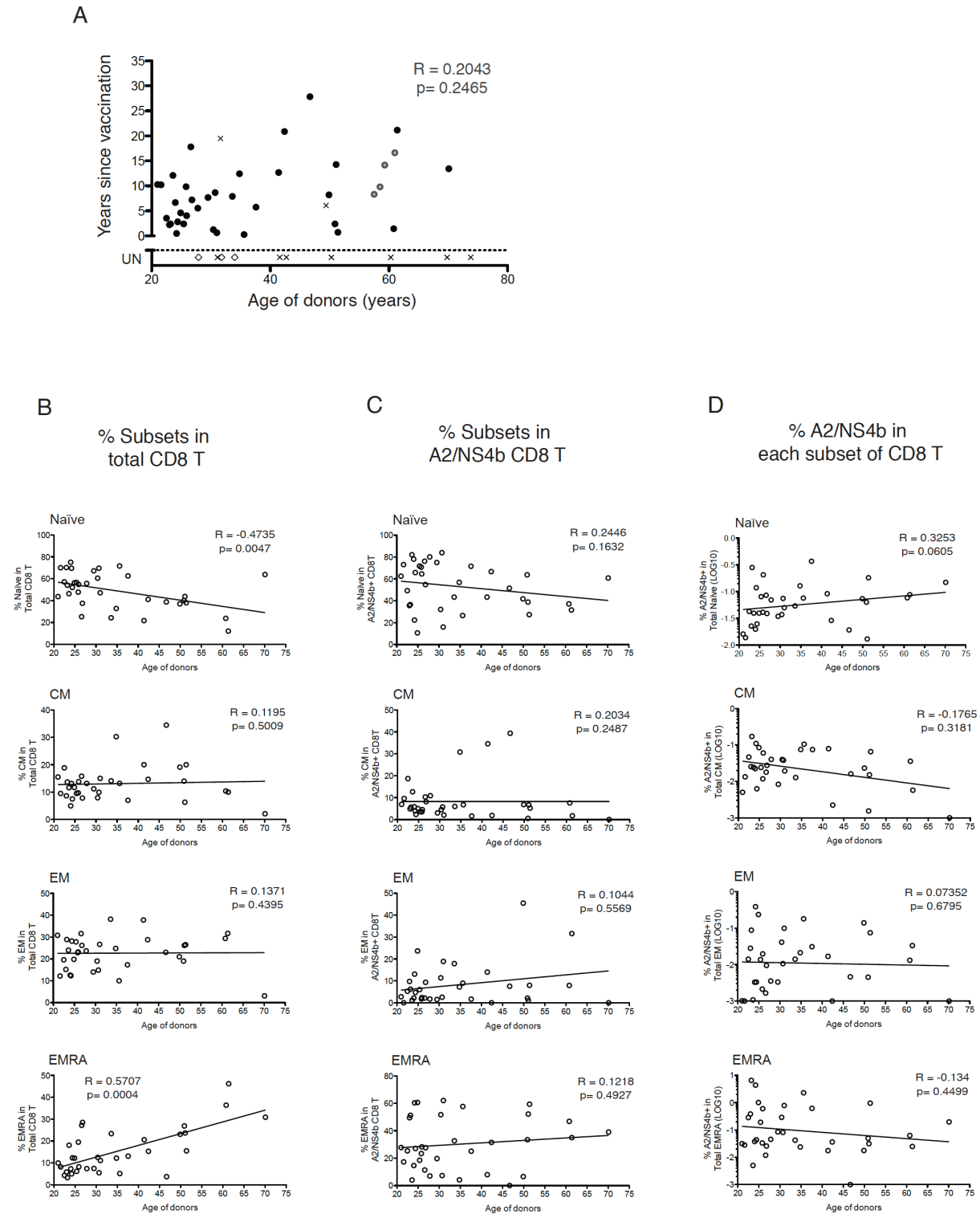

Fig. S1. Influence of inter-donor and age-related variability and its normalization for the study of A2/NS4b+ CD8 T cell subsets. A. "Years since vaccination" *versus* 'age of donors': donors with long vaccination history (especially >10 years) tend to be older. Symbols: ● = vaccinees (N=34); ◇ = unvaccinated controls (N=3); × = excluded donors (% A2/NS4b <0.01%); ◉ = vaccinees with multiple vaccines (N=4). R = Spearman correlation coefficient on the 'vaccinees' group. **B, C & D.** For the vaccinees group (N=34), the age of donors (x-axis) was plotted against the % of various differentiation subsets in Total CD8 T cells (C), against the % of various differentiation subsets in A2/NS4b+ CD8 T cells (D), and against the % of A2/NS4b+ cells within the various differentiation subsets (E). Spearman correlations R and best-fit lines are indicated.

Figure S2

A

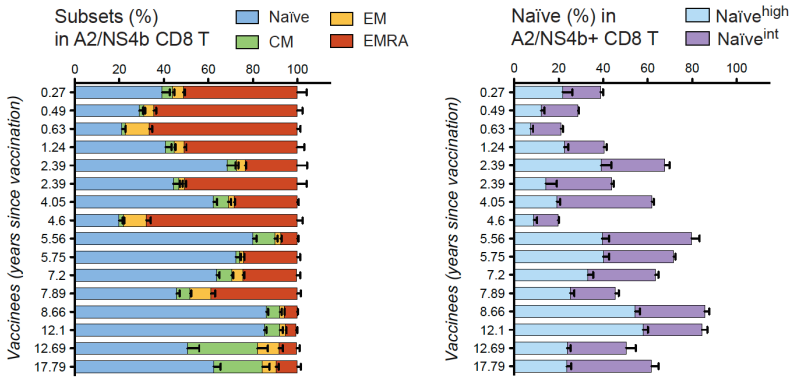

B

	Naïve		CM		EM		EMRA	
	Total	**A2/ NS4b+**	Total	**A2/ NS4b+**	Total	**A2/ NS4b+**	Total	**A2/ NS4b+**
CD27	99	98	94	97	70	79	46 ***	75
CD28	98	97	97	100	71 ***	50	22 ***	41
BTLA	92	88	78	86	56	58	53 ***	79
IL7Ra	92	97	90	94	63	55	31 ***	61
CD62L	65	62	40	36	16 ***	43	35 ***	51
CXCR3	48 ***	84	67 ***	87	25 ***	55	34 ***	60
IL2Rb	22 ***	58	61	70	72	72	81	82
ABC-B1	18	10	15	14	27	17	14	4
CD95	16 ***	80	98	96	98 *	85	95 ***	73
CD58	14 ***	73	91	87	99	99	98	99
CD38	13	19	6 *	19	8	18	6	18
CD11a^hi	10 ***	61	72 *	38	91 ***	64	95	86
KLRG1	10 ***	58	50 **	64	87	95	91	96
IL15Ra	9	11	3	4	1	4	4	3
CD25	8	7	4	2	3	2	5	5
2B4	8	15	50 ***	35	90 **	72	94 ***	62
CCR4	6	6	12	7	6	6	3	4
iGrnzA	6 ***	34	28 *	39	83	80	87	92
IL18Ra	5 ***	55	39	56	63	74	57 ***	75
CD45RO	4 ***	22	92	85	94	80	18	28
CD103	4	3	19 **	5	6	3	2	1
PDL1	4	5	4	9	3	6	4	3
CCR5	3	7	9	8	34 ***	14	12	10
GrznB	3	12	6	13	25 ***	73	50	52
ICOS	3	6	13	9	7	8	3	7
HLA-DR	3	7	12	6	20	11	20	9
CLA	3	10	19	14	13	16	9	4
CD161	3 *	14	22	17	48	48	27	37
CD69	2	4	1	1	2	1	2	1
iPFN	2	6	2	2	23	23	50 *	37
PD1	1	2	7	3	15	8	7	5
Overall =		**		ns		ns		ns

	A2/NS4b+ Naïve	
	Naïve-high	**Naïve-int**
CD27	99	97
CD28	99	96
BTLA	90	85
IL7Ra	98	96
CD62L	69 *	58
CXCR3	80	90
IL2Rb	48 ***	72
ABC-B1	16 *	5
CD95	69 ***	93
CD58	56 ***	90
CD38	23	16
CD11a	51 ***	66
KLRG1	43 ***	73
IL15Ra	17 **	4
CD25	10	4
2B4	8 ***	22
CCR4	8	4
iGrnzA	20 ***	47
IL18Ra	41 ***	66
CD45RO	15 ***	29
CD103	4	1
PDL1	4	5
CCR5	6	8
GrznB	12	12
ICOS	7	6
HLA-DR	5	8
CLA	7	12
CD161	8	18
CD69	6	2
iPFN	9	3
PD1	1	2
Overall =		ns

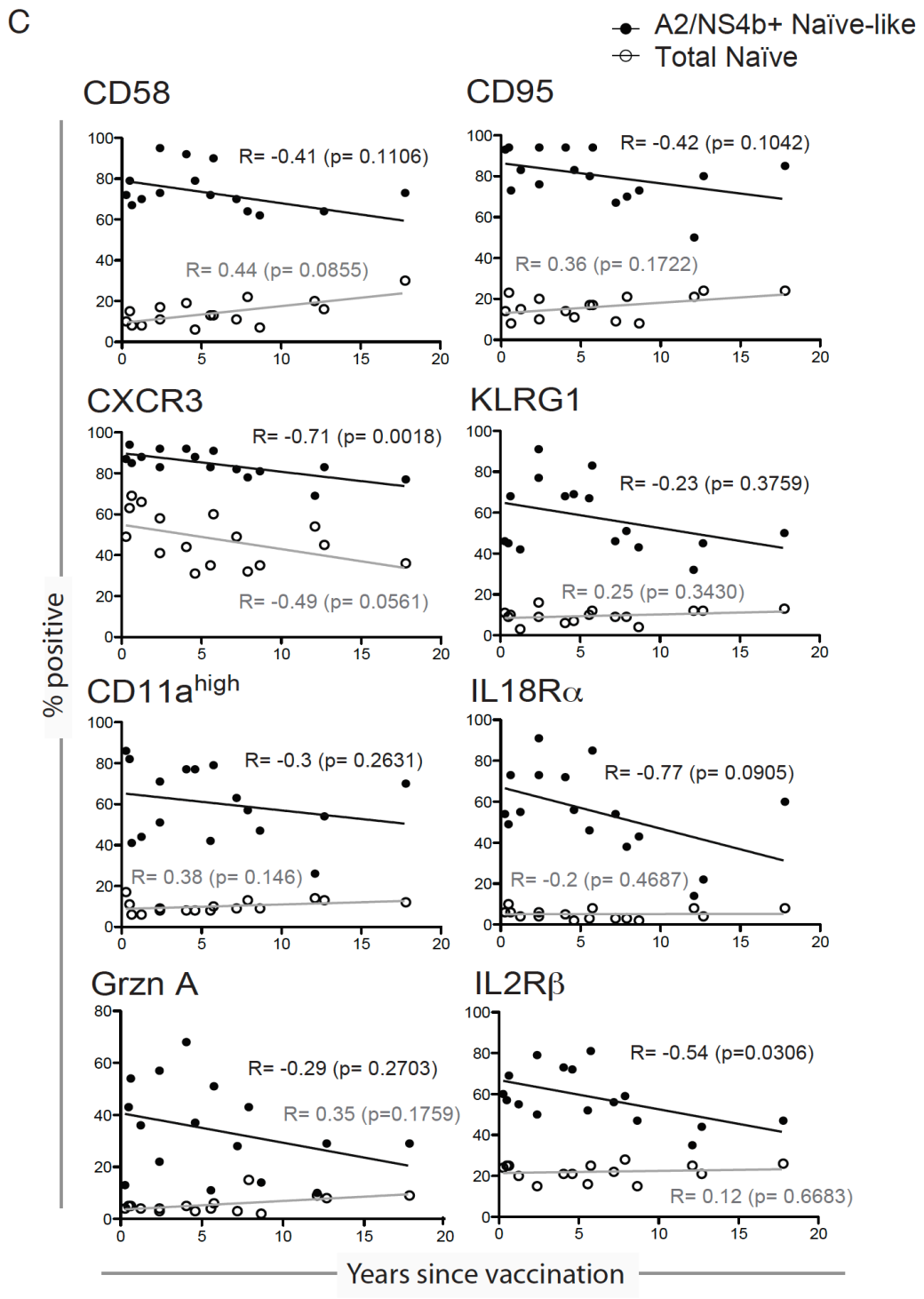

Fig. S2. Data complementary to fig. 3. A. Subset distribution in A2/NS4b+ CD8 T cells amongst the 16 vaccinees selected for in-depth studies (shown is the average and standard error of the analyses across the 9 staining panels used to assess the 31 markers). **B.** As in fig. 3 G and H, with additional data: a total of 31 markers, showing all detectable subsets within the A2/NS4b CD8 T cells. Cell populations below 20 events were not considered for marker analysis. While Naïve and EMRA subsets are generally predominant (fig. S2A), not all donors generated data for all populations. Bonferroni adjusted p-values following 2-way ANOVA are indicated per marker. Wilcoxon matched-pairs test to compare profiles "overall" are indicated at the bottom. **C.** Expression of markers in the Naïve-like phenotype of YF-specific CD8 T cells over the years post-vaccination. Shown are the eight markers that are most distinctly expressed in Naïve-like A2/NS4b+ CD8 T cells compared to Total Naïve, plotted *versus* the 'years since vaccination'. Spearman correlations R and best-fit lines are indicated.

Figure S3

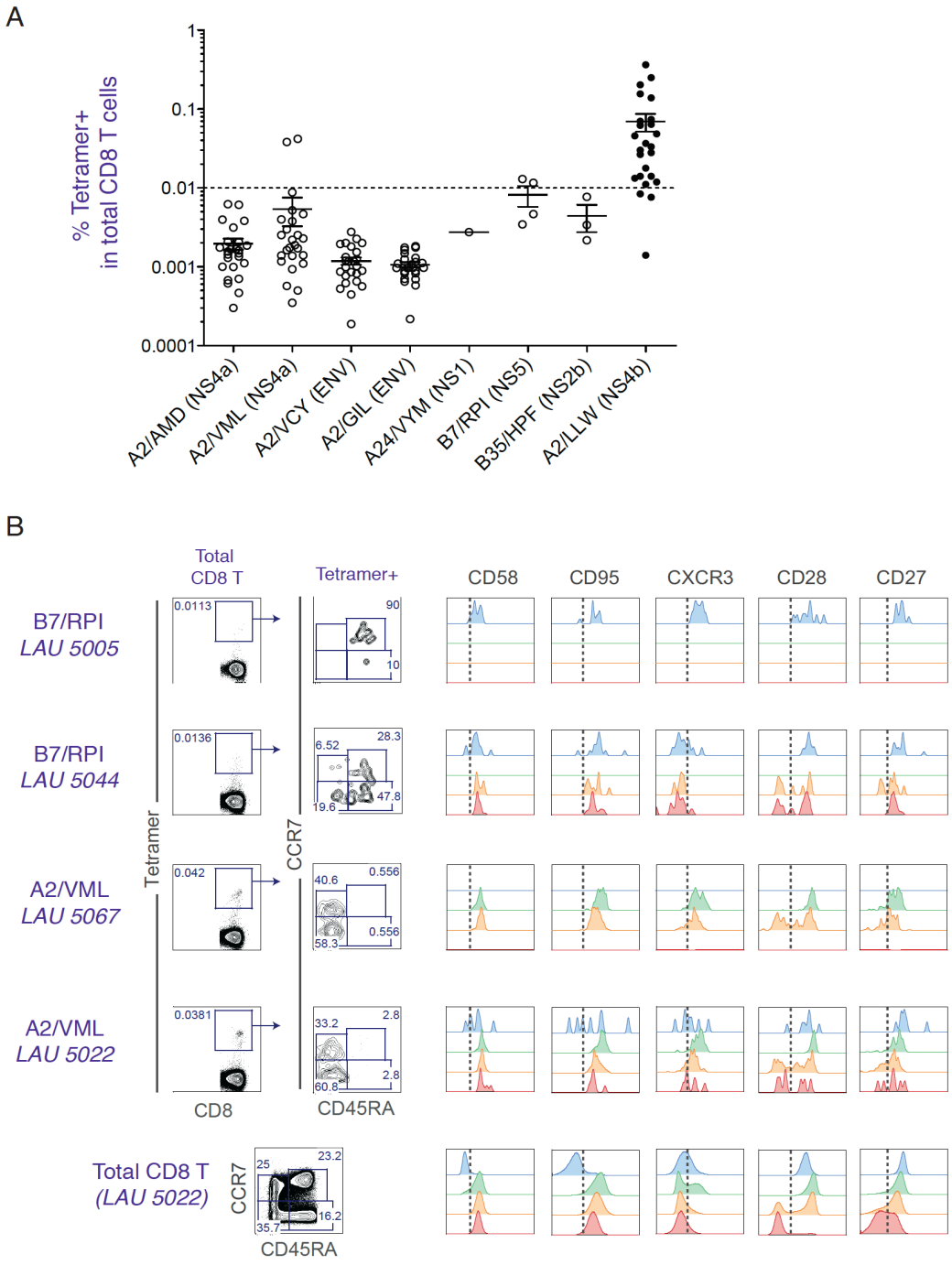

Fig. S3. Analyses of CD8 T cells specific for Yellow Fever epitopes alternative to the HLA-A*02-restricted NS4b. CD8 T cells from vaccinees (n=27, of which 2 HLA-A*02 negative) were analyzed for specificities alternative to HLA-A*02-restricted NS4b$^{214-222}$ ("A2/LLW") using tetramers, as follows: HLA-A*02/NS4a$^{23-31}$ ("A2/AMD", n=25), HLA-A*02/NS4a$^{54-62}$ ("A2/VML", n=25), HLA-A*02/ENV$^{59-68}$ ("A2/VCY", n=25) and HLA-A*02/ENV$^{347-355}$ ("A2/GIL", n=25); and non-HLA-A*02 restricted epitopes: HLA-A*24/NS1$^{167-175}$ ("A24/VYM", n=1), HLA-B*07/NS5$^{211-219}$ ("B7/RPI", n=4), HLA-B*35/NS2b$^{110-118}$ ("B35/HPF", n=3). **A.** Frequencies of tetramer positive cells in total CD8 T cells; the frequencies of A2/NS4b+ CD8 T cells (n=25) are indicated for comparison. The threshold for positive staining was 0.01%. **B.** Gating strategy used for the analysis of frequencies, subset distribution and staining for CD58, CD95, CXCR3, CD28 and CD27 of tetramer positive cells, showing the four positive samples (two A2/VML and two B7/RPI showed tetramer positive > 0.01%).

Figure S4

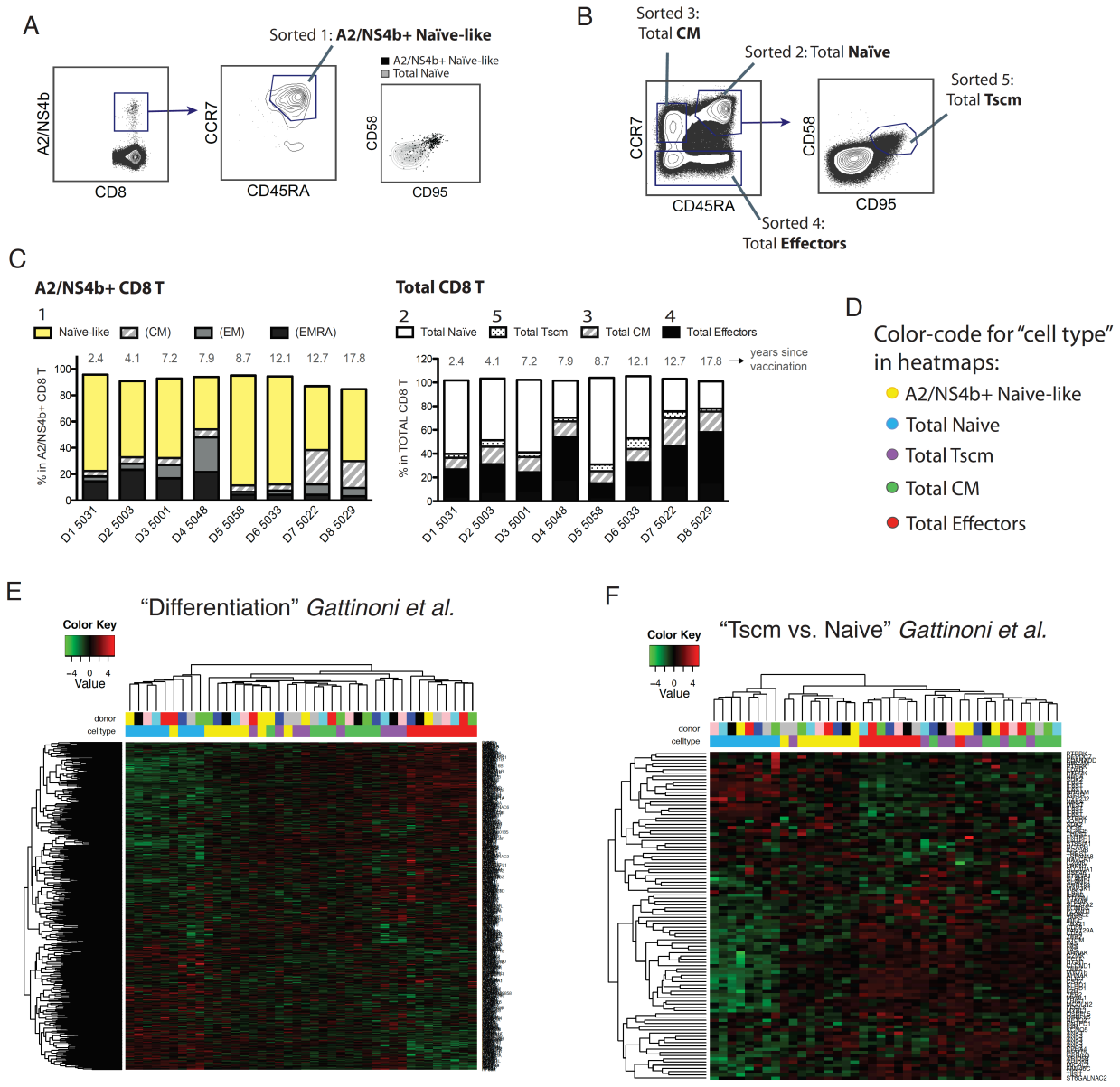

Fig. S4. Data complementary to fig. 5. A & B. Samples and sorting strategy for the purification of CD8 T cell subsets for mRNA analysis by whole genome microarrays. As shown in **A,** Naïve-like YF-specific CD8 T cells (population 1) were selected within total CD8 T cells based on A2/NS4b+ cells and further gating on CCR7+ CD45RA+ cells; these A2/NS4b+ Naïve-like CD8 T cells were checked for positive CD58 and CD95 expression, in contrast to the conventional Total Naïve population. The remaining populations were isolated from total live CD8 T cells (A2/NS4b tetramer negative), as shown in **B**, using conventional gating to select for Total Naïve (CCR7+ CD45RA+, population 2), Total CM (CCR7+ CD45RA-, population 3) and Total Effectors (CCR7-, population 4). Lastly, the recently described Tscm subset was isolated from the conventional Naïve gate (CCR7+ CD45RA+) by gating on the CD58+ CD95+ cells (population 5). **C.** Subset distribution of samples from the eight vaccinees selected (labeled D1 to D8 and their corresponding study number). **D.** Color-code for the populations shown in the heatmaps in E and F. **E and F**. Unsupervised clustering of the 40 samples (5 populations, n=8 donors) by interrogating the genesets described by Gattinoni et al. in their report of the Tscm subset *(23)*, corresponding to the "differentially regulated genes among CD8 T+ cell subsets" ("Differentiation", in G) and to the differentially regulated genes among Tscm and Naïve ("Tscm *versus* Naïve", in H). The degree of clustering and relatedness between samples is represented by the branching shown above the heatmap.

Figure S5

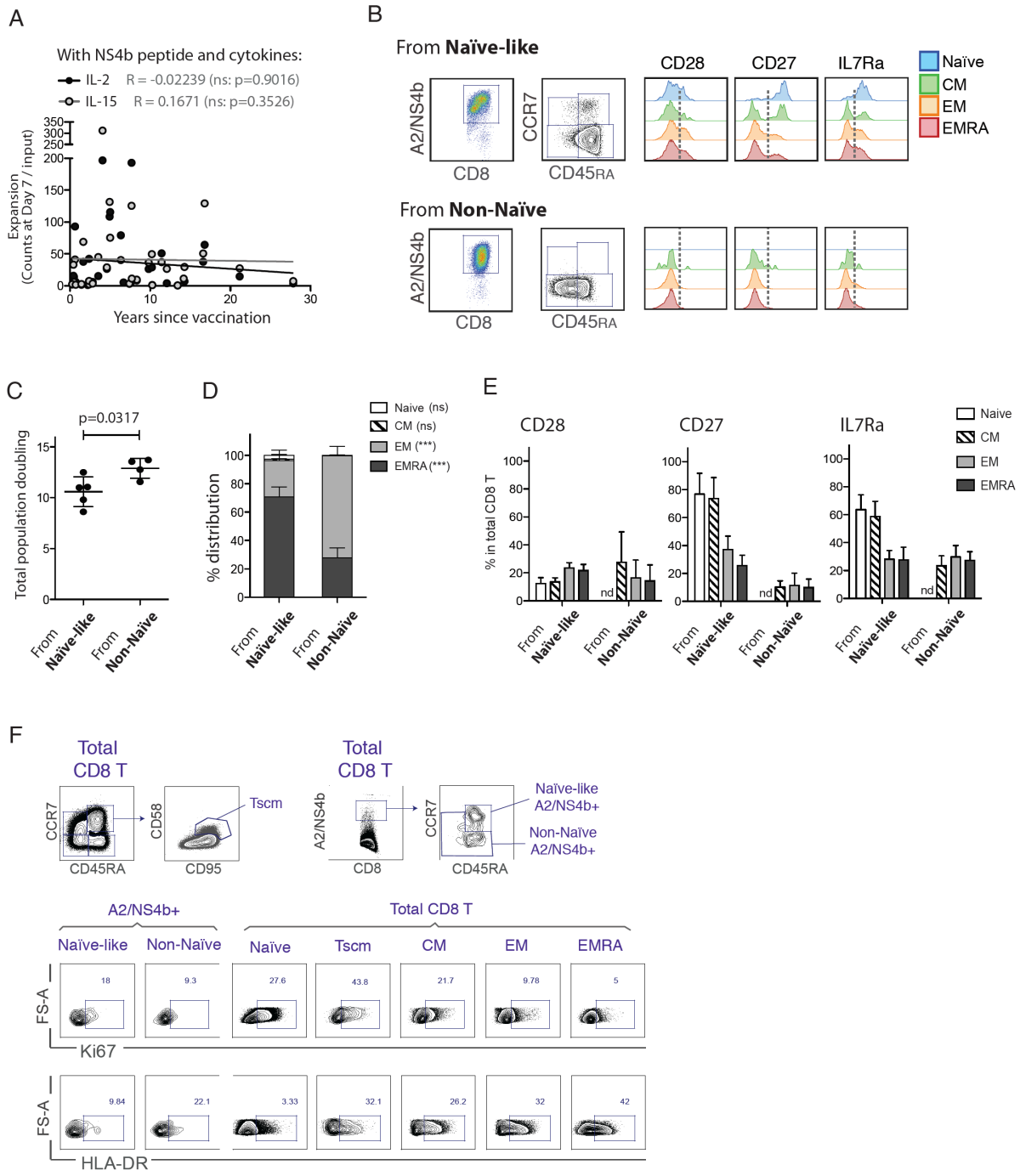

Fig. S5. Data complementary to fig. 6. A. 'Expansion' (data shown in fig. 6A: peptide + cytokines) related to the 'years since vaccination'. R = Spearmann correlation coefficients. **B to E.** Data complementary to the expansion of purified A2/NS4b+ CD8 T cells, Naïve-like or Non-Naïve, at day 14 (fig. 6 C to E). B: representative flow cytometry analyses of expanded cells. C: Total population doubling (mean, SD, and p-value from Mann-Whitney test). D: Subset distribution in expanded cells (mean, SEM, and p-values from 2-way ANOVA). E. Frequency of positive cells amongst the various subsets in expanded cells, for the three indicated markers (mean and SEM). **F.** Gating strategy for the analyses of CD8 T cells stimulated with anti-CD3 and anti-CD28 (fig. 6 F). Reference subsets were gated as in fig. 1 C; Tscm were gated as CD58+ CD95+ in the Naïve gate (note that the 24h stimulation resulted in upregulated CD95, as compared to unstimulated or 4h stimulation in fig. S6). NS4b-specific CD8 T cell subsets were gated as A2/NS4b+ and subsequent CCR7 and CD45RA discrimination, as indicated. The various populations were then assessed for Ki-67 and HLA-DR expression.

Figure S6

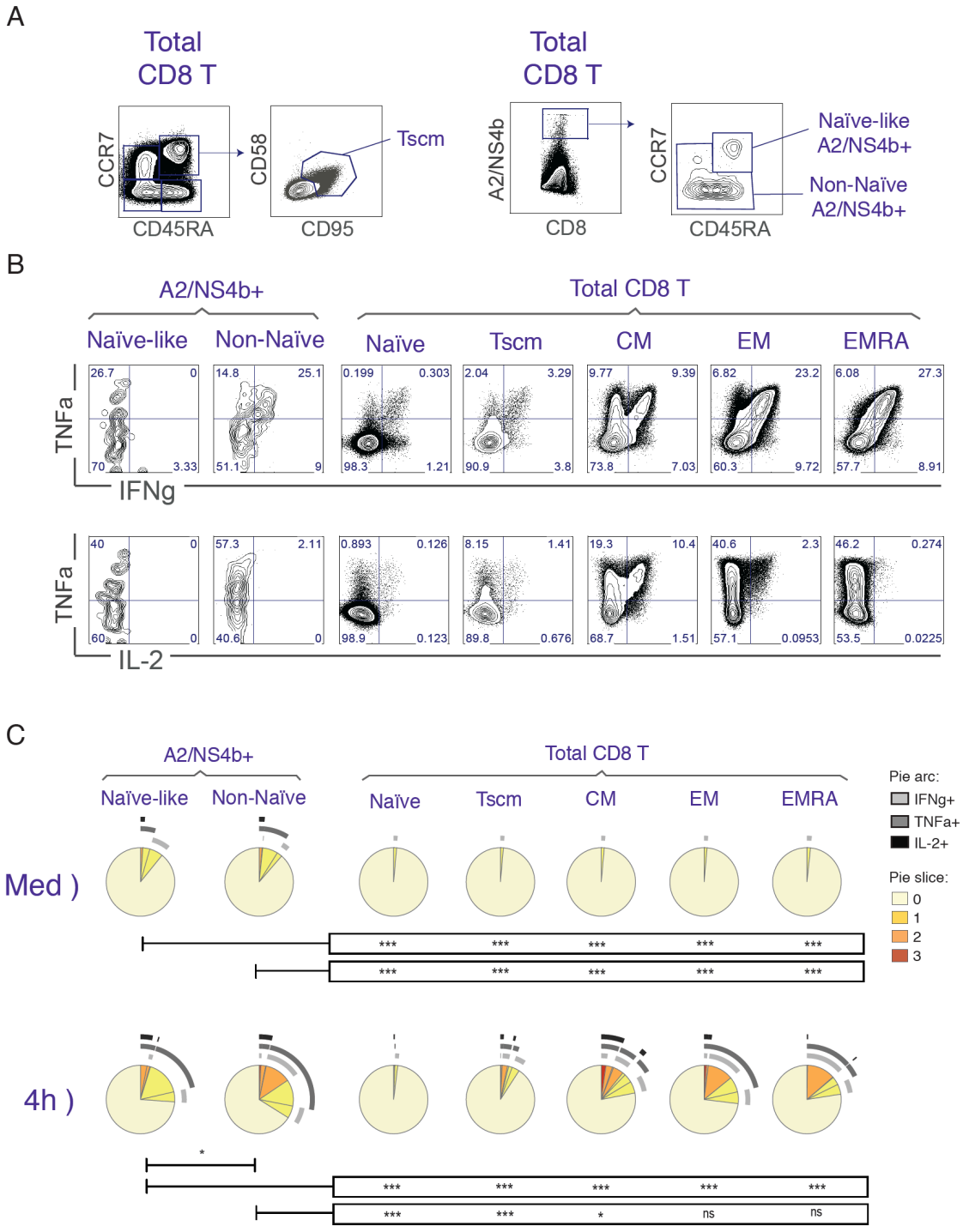

Fig. S6. Cytokine production by NS4b-specific CD8 T cell subsets in comparison the reference subsets in Total CD8 T cells. CD8 T cells from vaccinees (n=7) were stimulated with anti-CD3 and anti-CD28 beads for 4h. **A.** Gating strategy: the reference subsets were gated as aforementioned (fig. 1 C); Tscm were gated based on CD58+ CD95+ expression in the Naïve gate; A2/NS4b+ CD8 T cell subsets (Naïve or Non-Naïve) were gated based A2/NS4b+ signal and subsequent CCR7 and CD45RA discrimination, as indicated. **B.** Representative plots of the various populations assessed for intracellular cytokine production, including IFNγ, IL-2 and TNFα. **C.** Quantification of co-expression of cytokines (SPICE analysis), showing one pie chart with the average cytokine production per population and per treatment. Pie arcs and slices represent the percentage of cells positive for IFNγ, IL-2 and TNFα, as indicated in the legend.

Table S1. Summary of the cohort of Yellow Fever 17D vaccinees. Study identification code (LAU), age, gender, vaccination history (years) and frequencies of A2/NS4b+ in total CD8 T cells (donors in regular italic had frequencies below 0.01%).

LAU	Age	Sex	Years since vaccine	% A2/NS4b in CD8 T
5051	35.6	F	0.27	0.2030
5052	24.2	F	0.49	0.3650
5019	31.0	F	0.63	0.1390
5044	51.4	F	0.71	0.2510
5013	30.38	M	1.24	0.0703
5046	60.8	M	1.43	0.0492
5040	23.0	M	2.21	0.0447
5009	50.9	F	2.38	0.0399
5050	23.2	F	2.39	0.4150
5031	25.41	F	2.39	0.0638
5039	24.4	M	2.82	0.0200
5035	22.5	F	3.53	0.0483
5003	25.9	F	4.05	0.1750
5018	24.9	M	4.60	0.2020
5025	27.78	F	5.56	0.0485
5006	37.60	F	5.75	0.3230
5020	49.4	M	6.09	*0.0084*
5042	24.0	F	6.67	0.0192
5001	26.76	F	7.20	0.0266
5012	29.5	F	7.68	0.0309
5048	33.56	M	7.89	0.0301
5066	49.9	M	8.21	0.065
5058	30.71	F	8.66	0.0621
5057	25.75	F	9.82	0.0280
5014	21.6	F	10.21	0.0132
5036	21.0	F	10.26	0.0113
5033	23.57	F	12.10	0.0228
5067	34.8	M	12.43	0.074
5022	41.44	M	12.69	0.0458
5043	70.1	M	13.42	0.1560
5032	51.1	M	14.27	0.0141
5029	26.6	M	17.79	0.0280
5047	31.6	F	19.46	*0.0014*
5002	42.4	M	20.88	0.0178
5028	61.4	F	21.16	0.0333
5045	46.7	M	27.84	0.0141
5041	55.5	M	35.02	*0.0076*
5026	57.5	F	8.32 (34.05)	0.0119
5015	58.5	F	9.81 (22.05)	0.0133
5023	59.3	M	14.17 (25.47, 38.26)	0.0111
5024	61.0	M	16.61 (31.33)	0.0368

Table S2. Main genes contributing to PC1. Main positive and negative contributors in the PCA considering the top 10% variable genes.

PCA with Top 10% (Figure S6 A)

PC1: positive		PC1: negative	
Probe	Gene	Probe	Gene
A 23 P105957	ACTN1	A 33 P3243832	ZEB2
A 23 P343398	CCR7	A 24 P53976	GLUL
A 33 P3334398	CA6	A 23 P207564	CCL4
A 19 P00802168	AK123124	A 33 P3363933	FCRL6
A 21 P0012873	LOC100507387	A 33 P3354607	CCL4
A 32 P84373	FAM153A	A 23 P151294	IFNG
A 33 P3307253	AK5	A 23 P99275	KLRB1
A 24 P213788	LOC641518	A 24 P261760	KLRG1
A 21 P0007821	XLOC 009661	A 23 P142560	ZEB2
A 23 P30634	BACH2	A 23 P107744	S1PR5
A 23 P255896	C2orf89	A 33 P3285734	FCRL6
A 21 P0000787	LOC100507387	A 19 P00322571	MIAT
A 33 P3308512	SLC16A10	A 24 P129632	DLG5
A 24 P108863	SCML1	A 23 P209678	PLEK
A 23 P411723	PLAG1	A 23 P103803	FCRL3
A 21 P0000788	LOC100507387	A 21 P0000590	ZEB2
A 21 P0014082	LOC100507013	A 23 P68601	CST7
A 33 P3280801	LMO7	A 24 P173754	C1orf21
A 24 P143492	BCAS4	A 23 P119042	NKG7
A 21 P0008352	XLOC 010859	A 24 P268676	BHLHE40
A 23 P214627	AIF1	A 33 P3346891	MYBL1
A 23 P8834	EPHX2	A 33 P3209096	CD58
A 24 P20630	LEF1	A 33 P3327200	ATP2B4
A 21 P0008483	XLOC 011117	A 33 P3251369	GAB3
A 24 P85243	FAM153A	A 23 P1473	PRF1
A 21 P0014850	LOC100507427	A 24 P408740	CMC1
A 21 P0008484	XLOC 011117	A 19 P00318175	MIAT
A 23 P10025	NELL2	A 33 P3368334	FCRL3
A 23 P34375	TCEA3	A 23 P142447	MYO1F
A 23 P147465	PARK2	A 23 P146644	ANXA2
A 23 P80503	ROBO1	A 21 P0014596	LOC100506291
A 21 P0008385	XLOC 010924	A 24 P323114	ANXA2P3
A 33 P3344504	APBA2	A 24 P69095	ENC1
A 21 P0008486	XLOC 011117	A 33 P3879161	PIK3AP1
A 23 P120281	EDAR	A 24 P204244	ANXA2P1
A 21 P0008485	XLOC 011117	A 23 P204208	KLRD1
A 21 P0012276	SLC25A15	A 24 P233786	FAM129A
A 24 P30923	SNN	A 23 P124108	ITGAM
A 33 P3280805	LMO7	A 24 P54174	TNFRSF1B
A 24 P944253	KLHL6	A 21 P0000059	APOBEC3H
A 23 P149375	THEM4	A 33 P3354589	ENST00000378350
A 23 P78742	FLT3LG	A 33 P3342056	TIGIT
A 23 P56703	C2orf89	A 33 P3354604	ENST00000400702
A 32 P19806	DNAH11	A 23 P213562	F2R
A 24 P248053	TOP1MT	A 33 P3672482	USP28
A 24 P376760	CA6	A 23 P209954	GNLY
A 23 P138717	RGS10	A 21 P0014838	LOC100505471
A 33 P3329356	ENST00000512129	A 33 P3235213	TIGIT
A 21 P0000171	IL6R	A 33 P3274501	KLRF1
A 33 P3358731	PCSK5	A 33 P3376821	GZMA

Table S3. Differentially expressed genes comparing Naïve-like A2/NS4b+ CD8 T cells to the other four subsets listed. Adjusted *p* value = 0.05 (blue) and = 0.1 (orange).
Large table → provided as a separate excel file.

Table S4. Tetramers and antibodies used for Flow Cytometry analyses.
A) Tetramers

Tetramer			
HLA	peptide		context
	sequence	protein	
HLA-A*0201	LLWNGPMAV	NS4b$^{214-222}$	Yellow Fever virus
	AMDTISVFL	NS4a$^{23-31}$	
	VMLFILAGL	NS4a$^{54-62}$	
	VCYNAVLTHV	ENV$^{59-68}$	
	GILVTVNPI	ENV$^{347-355}$	
HLA-A*2402	VYMDAVFEY	NS1$^{167-175}$	
HLA-B*0701	RPIDDRFGL	NS5$^{211-219}$	
HLA-B*3501	HPFALLLVL	NS2b$^{110-118}$	
HLA-A*0201	ELAGIGILTV	Melan-A$^{26-35(A27L)}$	Melanoma
	GIGLGFVFTL	Matrix$^{58-66}$	Influenza
	GLCTLVAML	BMLF1$^{280-288}$	Epstein Barr Virus
	NLVPMVATV	pp65$^{495-503}$	Cytomegalovirus

All tetramers were purchased from TCmetrix Sarl (Epalinges, Switzerland).

B) Antibodies

Target	Fluorochrome	clone	Company	Staining
CD8	APC-Alexa750	B9.11	Beckman Coulter	surface
CCR7	Brilliant Violet or PE-Cy7	G043H7	Biolegend	
CD45RA	ECD	2H4LD11LDB9	Beckman Coulter	
	Alexa700	HI100	BD Biosciences	
CD16	Krome Orange	3G8	Beckman Coulter	
CD27	FITC	M-T271	BD Biosciences	
	APC-eF780	O323	eBioscience	
CD28	APC	CD28.2	BD Biosciences	
IL-7Ra/CD127	PerCP-Cy5.5	HCD127	Biolegend	
CD62L	PerCP-Cy5.5	DREG-56	Biolegend	
CD45RO	Alexa700	UCHL1	Biolegend	
ABC-B1/CD243	PE	UIC2	eBioscience	
FAS/CD95	PE-Cy7	DX2	Biolegend	
CD58	FITC or PE	1C3	BD Biosciences	
CD11a	PE-Cy7	HI111	BD Biosciences	
CD103	PE-Cy7	Ber-ACT8	Biolegend	
CLA	PE	HECA-452	Miltynei Biotec	
IL-2Rb/CD122	PE	Mik-B2	BD Biosciences	
IL-15Ra/CD215	PE	JM7A4	Biolegend	
IL-18Ra/CD218a	PE	444	Biolegend	
IL-2Ra/CD25	PE-Cy7	BC96	Biolegend	
CD38	Alexa700	HIT2	eBioscience	
CD69	FITC	FN50	BD Biosciences	
HLA-DR	FITC or PerCP-Cy5.5	L243	Biolegend	
ICOS	FITC	C398.4A	Biolegend	
PD1	PerCP-eF710	eBioJ105	eBioscience	
PDL1	PE-Cy7	MIH1	eBioscience	
2B4	PE-Cy5.5	C1.7	Biolegend	
KLRG1	A488	13F12F2	*in house* (H. Pircher)	
BTLA	PE-Cy7	BTLA7.2	Beckman Coulter	
CD161	PE-Cy7	HP-3G10	Biolegend	
CCR4	PerCP-Cy5.5	TG6	Biolegend	
CCR5	PerCP-Cy5.5	HEK/1/85a	Biolegend	
CXCR3	PerCP-Cy5.5	G025H7	Biolegend	
Ki-67	PE	Ki-67	Biolegend	
IFNg	PE	4S.B3	BD Biosciences	intracellular
IL-2	PerCP-Cy5.5	MQ1-17H12	BD Biosciences	
TNFa	Alexa700	HIT2	eBioscience	
Granzyme A	Alexa700	CB9	Biolegend	
Granzyme B	ECD	GB11	Molecular Probes	
Perforin	FITC	dG9	Ancell	